National Institute for Public Health
and the Environment
Ministry of Health, Welfare and Sport

A comparison of jet fire models

for horizontal two-phase and liquid releases

RIVM report 620550005/2012

E.S. Kooi | P.A.M. Uijt de Haag

National Institute for Public Health
and the Environment
Ministry of Health, Welfare and Sport

A comparison of jet fire models

for horizontal two-phase and liquid releases

RIVM Report 620550005/2012

Colophon

E.S. Kooi
P.A.M. Uijt de Haag

Contact:Eelke Kooi
eelke.kooi@rivm.nl

This investigation has been performed by order and for the account of the Ministry of Infrastructure and the Environment, within the framework of Development of QRA Guidelines (M/620550/10/RI)

Abstract

A comparison of jet fire models for two-phase and liquid releases

If a leak occurs in a pressurised pipeline with flammable liquids or gas, ignition will give rise to a jet fire. In the Netherlands, industries working with large quantities of hazardous substances are obliged to specify the minimum distance between these companies and surrounding buildings. How these distances should be calculated and which model to use, is laid down in legislation. The use of an alternative model requires approval from the Minister of Infrastructure and the Environment. The reliability, public nature and availability of the alternative model are important aspects in this assessment.

Shell model as an alternative
As commissioned by the Ministry of Infrastructure and the Environment, the National Institute for Public Health and the Environment (RIVM) has investigated whether or not the Shell jet fire model is more reliable than the prescribed model for a specific location in The Netherlands. This turned out to be true. As a result, an important condition for using the model for permit application has been met. Other requirements, such as the public nature and availability of the model, were not part of this investigation.

The reason for comparing models was the suspicion that the use of the prescribed jet fire model might have induced unfounded salvaging requirements. Therefore, the permit holder brought the outcomes of the legal model and the associated consequences up for discussion. With the Shell model, the distances would be 10 to 20 percent smaller. The use of the Shell model could also lead to smaller distances around other sites where two-phase and liquid jet fires determine the overall risk.

Method used
For this investigation we compared the complexity of the models and the quality of the validation. It turned out that the Shell model is derived from a larger set of data from experiments. In five selected cases the outcomes of the Shell model corresponded better to the measured values than the legal model.

Keywords:
QRA, jet fire, consequence, modelling

Rapport in het kort

Vergelijking van fakkelbrandmodellen voor vloeistoffen en tot vloeistof verdichte gassen

Als een leiding met brandbare vloeistof of gas onder druk beschadigd raakt, ontstaat bij ontsteking een fakkelbrand. In Nederland zijn industrieën die met grote hoeveelheden gevaarlijke stoffen werken verplicht om aan te geven wat de minimale afstand is tussen deze bedrijven en de omliggende bebouwing. In wetgeving is vastgelegd hoe deze afstand berekend moet worden en met welk rekenmodel. Voor het gebruik van een alternatief model is toestemming van de Minister van Infrastructuur en Milieu nodig. Belangrijke afwegingen hierbij zijn de betrouwbaarheid, openbaarheid en beschikbaarheid van het alternatief.

Shell-model als alternatief
Op verzoek van het ministerie van Infrastructuur en Milieu (IenM) heeft RIVM onderzocht of het fakkelbrandmodel van Shell voor een locatie in Noord-Holland betrouwbaarder is dan het voorgeschreven model. Dit blijkt inderdaad het geval. Daarmee is voldaan aan een belangrijke voorwaarde voor een eventueel gebruik van het model bij de vergunningaanvraag. Overige aspecten, zoals de openbaarheid en beschikbaarheid van het model, vallen buiten het bestek van dit onderzoek.

Aanleiding voor de vergelijking was het vermoeden dat er door het gebruik van het wettelijke fakkelbrandmodel bij de genoemde locatie mogelijk onnodig zou moeten worden gesaneerd. De vergunninghouder stelde daarop de uitkomsten van het wettelijke model en de daaraan verbonden consequenties ter discussie. Met het Shell-model zouden de afstanden 10 tot 20 procent kleiner zijn. Ook bij andere locaties waar het risico bepaald wordt door fakkelbranden van vloeistoffen en tot vloeistof verdichte gassen, kan het gebruik van het Shell-model leiden tot kleinere afstanden.

Werkwijze onderzoek
Voor het onderzoek zijn de complexiteit van de rekenmodellen en de kwaliteit van de validatie vergeleken. Het model van Shell blijkt te zijn gestoeld op een grotere hoeveelheid data uit experimenten. Voor vijf geselecteerde cases kwamen de uitkomsten van het Shell-model beter overeen met de gemeten waarden dan de uitkomsten van het wettelijke model.

Trefwoorden:
QRA, fakkelbrand, effecten, modellering

Contents

List of figures and tables

Figures

Tables

Summary

In this report three jet fire models were compared. The motivation for this investigation was a claim by the Nederlandse Aardolie Maatschappij (NAM) that the jet fire model that is prescribed by the Dutch legislation, produces outcomes that are inaccurate and overconservative for specific cases. As a result, the use of this model would have undesirable consequences for permit application and land-use planning, in particular for the NAM site in Den Helder.

The scope of this study was limited to jet fires related to mixed gaseous and liquid releases. These jet fires are most relevant for the permit application for the NAM site in Den Helder and for the land-use planning around this site. For the assessment of the consequences of such jet fires, the legislative authorities currently prefer to use the JFSH-Cook model that is implemented in SAFETI-NL. NAM claimed however that the Cracknell model from Shell would give a more reliable prediction of the consequences of these jet fires. A third model, the Barker model from Shell, was investigated for reasons of completeness.

The investigation which model produces the best results comprised of three parts. Firstly, the physical assumptions behind the models, the amount of validation data and the quality of the validation data were assessed. Subsequently, the outcomes of the models were compared against five relevant jet fire experiments. Lastly, the quality of the model outcomes outside the validation range was investigated by comparing the outcomes with general knowledge from literature.

The outcome of the investigation was that the Shell models produce more reliable results and that the outcomes of the JFSH-Cook model are expected to be overconservative for the considered releases. The Shell models are more sophisticated and are derived from a larger set of experimental data. When compared to realistic cases, the Shell models produced better outcomes than the JFSH-Cook model. Lastly, the model predictions of the Shell models in the extrapolated range were deemed more reliable.

Overall, the Cracknell model is expected to produce the best results for the jet fire scenarios that are deemed most relevant for the NAM site in Den Helder. When using the Cracknell model, the expected consequences of these scenarios are more limited than when using the JFSH-Cook model. The use of JFSH-Cook model could therefore lead to restrictions for the permit application and land-use planning that are undesirable and also unnecessary from a scientific point of view.

However, legislative authorities may have other requirements for the use of jet fire models in the permit application and land-use planning, such as the availability of these models for third parties and a description of these models in the open literature. These aspects were not investigated in this study.

1 Introduction

The aim of this project is to verify a claim, made by the Nederlandse Aardolie Maatschappij (NAM), that the jet fire models in FRED™ give a better prediction of effect zones for heat radiation than the jet fire models in SAFETI-NL™. In order to verify this claim, model outcomes from FRED and SAFETI-NL are compared to experimental data. In addition to available experimental data, information on jet fire properties and effect zones in the open literature are also addressed. If NAM is right, the FRED models will give a better fit to the experimental data than the models in SAFETI-NL.

Specific attention will be paid to the release scenarios that are prescribed for the Quantitative Risk Assessment (QRA) for the Den Helder site of NAM. These scenarios involve horizontal releases of mixtures containing various hydrocarbons varying from C1 to C9 at high pressure (40 to 80 bar) from large diameter pipes (36 to 48”). In order to verify to which extent the jet fire models can be applied to these release scenarios, a detailed description of the model assumptions and model validation is needed. If the calculated effect zones using the models mentioned above differ significantly, it must be decided which of the models can best be used for the prediction of effect zones at the Den Helder site.

This report consists of the following parts:

In chapter 2 the various jet fire models will be described. The description includes the flame geometry, the surface emissive power of the flame and the total fraction of heat radiated. The description also includes an overview of the amount of data used to design or validate the model, the validation range and the quality of the fit of the key parameters in the model.

In chapter 3 the LPG jet fire model in FRED, the generic two-phase and liquid release model in FRED and the two-phase and liquid release model from SAFETI-NL will be compared to a limited set of experimental jet fire releases for which sufficiently detailed data were available. This comparison includes two jet releases performed by Shell and three releases performed by British Gas.

In chapter 4 it will be analysed to which extent the jet fire models can be used for the QRA scenarios for the NAM Den Helder site. These release scenarios differ significantly from the experimental data used in chapter 3. More specifically, the NAM Den Helder release scenarios involve mixtures of hydrocarbons ranging from C1 to C9 and release rates which are two orders of magnitude higher than the release rates for which experimental data are available. One Den Helder release scenario is selected for further comparison and the corresponding outcomes of the jet fire models in FRED and SAFETI-NL are presented. Subsequently, the model outcomes are compared to the reported behaviour of two-phase and liquid hydrocarbon releases in the literature. This comparison with literature will provide further insight in the applicability of the FRED and SAFETI-NL models for the NAM Den Helder QRA scenarios.

In chapter 5 general conclusions will be drawn on the applicability of the FRED and SAFETI-NL models for the NAM Den Helder QRA scenarios discussed in this report. If the calculated effect zones using these models differ significantly, we will substantiate which model is expected to give the best prediction of the size of effect zones.

The current study only comprises an assessment of the quality of the models and the expected accuracy of the model outcomes. This does not imply that the model that is expected to give the best predictions will automatically be selected as the model that should be used for third party risk calculations for the NAM Den Helder site or for Dutch establishments with flammable substances in general. Such a decision depends on several other factors as well, including transparency, which are not addressed in this report. Furthermore, it was decided earlier that a full bore rupture of one of the fingers of the slugcatcher had to be included as one of the QRA scenarios. The possibility of this event is currently taken as a premise and its likelihood is not further discussed in this report.

All outcomes for FRED and model descriptions for FRED apply to version 5.0.0. All outcomes for SAFETI-NL and model descriptions for SAFETI-NL apply to version 6.5.3. PHAST 6.5.3 was used for the JFSH-Cook consequence analyses in chapter 3.

This comparison was carried out by the Centrum Externe Veiligheid (Centre for External Safety) of RIVM and was commissioned by the Dutch Ministry of Infrastructure and Environment. The description of the models in FRED and the validation behind these models (see chapter 2) is largely provided by Shell Global Solutions (SGS). The description of the models in SAFETI-NL and the validation behind these models (also chapter 2) was done by RIVM together with DNV. Additional data reports were provided by GL Noble Denton (formerly Advantica) and the Steel Construction Institute. Stakeholders (notably NAM, SGS and DNV) have been invited to comment the comparison.

2 Description of the models and their validation

2.1 Introduction

The model comparison is carried out for the Barker LPG jet fire model, the Cracknell generic two-phase and liquid jet fire model and the JSFH Cook model for two-phase and liquid jet fires. The first two models are implemented in Shell FRED, the latter is implemented in SAFETI-NL.

This chapter provides a qualitative description for each of the selected models. This includes:

- a description of the flame shape and orientation;
- a list of parameters that determine the flame shape, orientation and fraction of heat radiated;
- a qualitative description of the influence of each of these parameters;
- insight in the amount of data used for validation, the validation range and the quality of the fit of the key parameters.

The use of SAFETI-NL is prescribed for establishments that are within the scope of the BEVI legislation ([1]). Therefore, the JFSH-Cook model in SAFETI-NL is regarded as the point of departure and will be discussed first. The FRED models will be discussed in section 2.3 and 2.4. A first comparison of the quantitative behaviour of the models will be presented in section 2.5 followed by a summary of the first findings in section 2.6.

2.2 Description of the JFSH-Cook model as implemented in SAFETI-NL

The two-phase and liquid jet fire model that is implemented in SAFETI-NL is described in detail in the 'JFSH Theory Document' on the SAFETI-NL installation CD ([2]). The model is derived from a model published by Chamberlain ([3]) in 1987, for which modifications were proposed by Cook, Bahrami and Whitehouse ([4]) in order to account for two-phase and liquid jets. The corresponding outcomes have been validated against publicly available experimental data from Bennett, Cowley, Davenport and Rowson ([5]) and Selby and Burgan ([6]).

The model may be used for flammable substances that are two-phase or liquid after depressurisation to ambient pressure, though the user is advised to verify if the modelled release conditions are in the validation range (see section 2.2.2). For the input data, such as discharge rate and final velocity, the model depends on discharge variables that are calculated elsewhere in the software.

The two-phase and liquid model that is currently implemented in SAFETI-NL deviates from the initial proposal by Cook, Bahrami and Whitehouse ([4]). In agreement with the terminology of DNV it will nevertheless be referred to as the JFSH-Cook model.

For reasons of completeness it is noted that the implementation of the JFSH-Cook model in SAFETI-NL has restrictions that do not pertain to the commercially available counterparts of SAFETI-NL, PHAST and PHAST Risk.

2.2.1 Qualitative description of the model

2.2.1.1 Flame shape and orientation

The flame geometry is depicted in Figure 1. The flame shape is approximated with a tilted frustum of a cone. The modelled flame shape has the following features:

- The flame starts at a distance B from the orifice (along the release direction). This 'lift off distance' is used for vertical and also non-vertical releases.
- The flame length, L_B, is equal to the distance between the orifice and the flame end (tip of the frustum at the flame axis).
- The length of the frustum, R_L, represents the length of the burning flame (along the flame axis).
- The width of the frustum base, W_1, represents the width of the burning flame near the orifice.
- The width of the frustum tip, W_2, represents the width of the burning flame at the flame end.
- θ_j is the angle between the release direction and the horizontal (jet angle).
- α is the angle by which the flame is deflected from the release direction due to wind impact.

For non-horizontal releases, the angle between the flame and the horizontal may increase or decrease due to wind effects. For horizontal releases, the flame direction is always horizontal. In particular the JFSH-Cook model does not take into account flame lift off due to buoyancy effects. Furthermore, there is no interaction between the modelled flame and the ground. Part of the modelled frustum may have a negative z-coordinate, in which case a warning and/or error is issued.

According to the Dutch guidelines for third party risk calculation ([1]) releases from aboveground pipelines should always be modelled as (along wind) horizontal releases, for which case both θ_j and α are equal to 0. In the related software tool PHAST (also owned and developed by DNV) it is possible to take into account crosswind effects on jet fires.

The flame length in the JSFH-Cook model is determined by the wind speed, the effective source diameter of the release and the Richardson number. The Richardson number represents the ratio of buoyancy and momentum forces and is proportional to the third root of the ratio $g/(m \bullet v_j)$, in which g is gravitational acceleration, and $m \bullet v_j$ the momentum of the jet (derived from the expanded jet velocity).

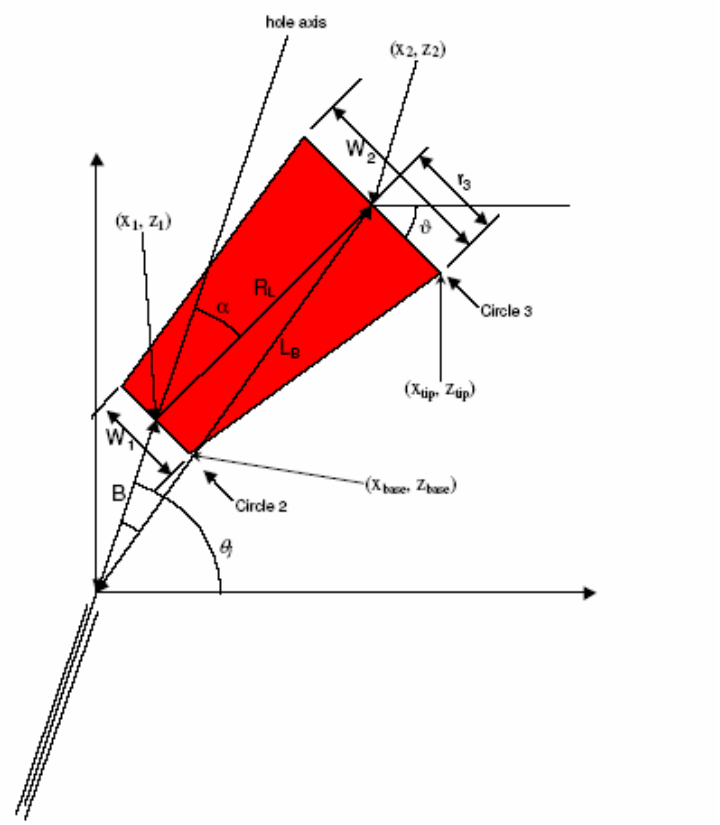

Figure 1 Geometry of the JFSH-Cook model in SAFETI-NL.

The features above were already present in the Chamberlain model for gaseous releases ([3]). For two-phase and liquid releases, the following rules are defined in the JSFH-Cook model:

- Following a recommendation of PHAST users in 1998, the amount of mass involved in the jet is set at three times the vapour mass after rainout (with the total release rate as an upper limit). This assumption is expected to give a better prediction of flame lengths for liquid releases but has not been verified with experiments. *Note: this assumption does not apply to the 'stand-alone model' which is available in PHAST. However, as the current study focuses on SAFETI-NL, the stand-alone models will not be discussed.*
- The effective diameter of the release is linear with $(\rho_j/\rho_{sv})^{0.5}$, in which ρ_j is the density of the jet after expansion to atmospheric pressure and ρ_{sv} is the saturated vapour density at the orifice. For pure gas releases the corresponding factor was $(\rho_j/\rho_{air})^{0.5}$, ρ_{air} being the density of ambient air. According to the JFSH theory document ([2]) this gives an effective diameter that - in conjunction with the release rate - produces an expanded jet velocity that is equal to the expanded jet velocity had it been a pure gas release.

The lift off distance is equal to 1.5% of the flame length for all horizontal two-phase and liquid releases. As the release direction is equal to the flame direction (in accordance with the Dutch guidelines), the frustum length amounts to 98.5% of the flame length.

The width of the flame at the base (W_1) is very similar to the width of the frustum in the Chamberlain model ([3]). It depends on the ratio of wind speed and expanded jet velocity, the effective release diameter and the Richardson number (buoyancy versus momentum). The width of the flame at the top (W_2) is taken entirely from the Chamberlain paper, and depends on the flame length and the ratio of wind speed and expanded jet velocity.

2.2.1.2 Surface emissive power and fraction of heat radiated

The surface emissive power is derived from the total amount of heat radiated and the total surface area of the flame. For fuels with a molecular weight (M_W) lower than 21 kg/kmol, the fraction of heat radiated is taken from the Chamberlain paper ([3]) and depends only on the expanded jet velocity. The fraction of heat radiated diminishes from 0.32 for low velocity releases, to 0.11 for high velocity releases. For heavier fuels, the fraction of heat radiated calculated with the Chamberlain correlation is increased by a factor $(M_w/21)^{0.5}$, using an upper limit of 1.69 for this factor. Overall the fraction of heat radiated may thus vary from 0.54 for heavy hydrocarbons released with low pressure, to 0.11 for methane at (very) high pressure.

The surface emissive power itself also has an upper limit, which is set at 400 kW/m^2 in SAFETI-NL. If the surface emissive power is capped, the fraction of heat radiated is decreased correspondingly.

2.2.2 Validation of the model

The JFSH-Cook model is a theoretical extension to the Chamberlain vapour jet model ([3]). In other words, the model is not based on experimental data directly. However, the model has been validated afterwards, against field data from 'Project AA' ([5]) and from 'phase 2 of BFETS' ([6]). The Project AA data involve horizontal free jets and horizontal impinging jets of natural gas and LPG. The free LPG releases are used for the validation of the JFSH-Cook model. The BFETS-2 data involve horizontal free jets and horizontal impinging jets of stabilised light crude oil and mixtures of stabilised light crude oil and natural gas. The releases of crude oil with no added natural gas were used by DNV for validation of the JFSH-Cook model.

A complete description of the validation is given in the JFSH theory document ([2]). Some difficulties were met by DNV because the jet fire model needs expanded jet velocity and temperature as input while the data reports only specify stagnant temperature and pressure. Another problem was that the composition of the crude oil could not be derived accurately from [6]. Moreover, at the time of the validation, the software (PHAST, PHAST Risk and SAFETI-NL) did not have a multi-component release model. Therefore, n-octane was used by DNV as a substitute for crude oil. Whether releases of mixtures can be accurately modelled with pure components will be further discussed in the text box 'Accuracy of the models for releases of mixtures' on page 27[(1)].

An overview of the number of releases used for the validation of the JFSH-Cook model is given in Table 1. The table also lists which stagnant pressures,

[1] Based on a temperature-recovery table reported by Selby and Burgan in [6], it was estimated by RIVM that about 10 wgt% of the crude oil consisted of C6-C8 hydrocarbons, and about 90% C9-C20. The temperature of 50% (vapour) recovery was 317°C and the temperature of 100% (vapour) recovery 345°C indicating that about half of the crude was C18-C20).

orifice diameters and release rates were used in the experiments. The table applies both to the validation of the flame shape (size and geometry) and the validation of the surface emissive power.

Table 1 Data used for validating the flame shape [(1)] in the JFSH-Cook jet fire model.

Released substance	*Number of releases used for validation*	*Range of stagnant pressures*	*Range of orifice diameters*	*Range of release rates*
LPG (97% propane)	5	6.3 - 9.7 bar(g) drive pressure	10 - 52 mm	1.5 - 18.0 kg/s
Stabilised crude oil	2	7 - 20 bar(g) stagnant pressure	14 - 18 mm	5.0 kg/s

(1) The flame shape includes the frustum length, width of the frustum base and the width of the frustum tip.

More information on the validation of the model is presented in Annex 1.

2.3 Description of the Barker LPG jet fire model as implemented in FRED

(The larger part of the text in this section was provided by Shell Global Solutions)

The Barker LPG jet fire model is implemented in FRED for two-phase releases of propane, butane and LPG. A full description of the model is provided in ([7]). The model can be applied to all releases of (mixtures) of propane and butane with a significant amount of liquid at the orifice. A warning is issued if the discharge rate or the exit velocity is outside the validation range.

2.3.1 Qualitative description of the model

Typical flame shapes observed during experimental pressurized releases of liquid LPG (propane and butane) have a flame region dominated by initial horizontal momentum followed by a flame region dominated by buoyancy. A flame shape model was developed to represent this observed behaviour consisting of a horizontal cone frustum to model the momentum dominated region attached to a tilted cylinder to model the buoyancy dominated part of the flame.

The intended application of the model is for liquid releases of LPG through an orifice or open pipe system driven either at saturated LPG pressure or a modest drive overpressure. The experimental test programme covered LPG mass flow rates up to 22 kg/s through maximum hole sizes of 52 mm.

2.3.1.1 Flame shape and orientation

The flame of the Barker LPG jet fire model has a horizontal part shaped like a frustum of a cone, and a tilted part shaped as a cylinder. The general flame shape including orientation is displayed in Figure 2. This (two-component) flame shape represents the 50% occurrence of the flame.

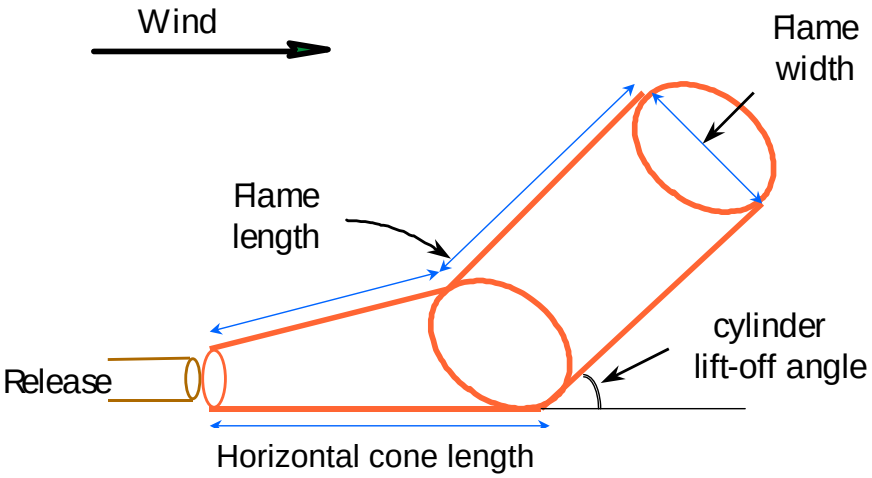

Figure 2 Flame shape for the Barker LPG jet fire model.
Diagram obtained from Shell Global Solutions

The flame shape is characterised by the following parameters:
- horizontal cone length;
- width of the frustum base;
- width of the frustum tip (flame width);
- flame length;
- lift-off angle.

The horizontal cone length is determined by the exit velocity and release diameter. The width of the frustum tip is determined by mass flow rate, wind speed, release diameter and density. Increases in mass flow rate and release diameter both give wider flames. An increase in wind speed results in narrower (and thus lower) flames. The (total) flame length is determined primarily by mass flow rate of the release. The lift-off angle is determined by the wind speed, flame width and density. In the absence of wind, the lift-off angle is roughly 60°.

2.3.1.2 Surface emissive power and fraction of heat radiated

The surface emissive power is determined by the temperature and amount of soot loading in the flame. For propane the surface emissive power is restrained by a maximum of 230 kW/m^2. For butane the surface emissive power is restrained by a maximum of 255 kW/m^2. The fraction of heat radiated is calculated from the SEP, the surface area of the flame and the overall combustion power.

2.3.2 Validation of the model

An overview of the number of releases used for developing the Barker LPG jet fire model is given in Table 2. The table also lists which orifice pressures, orifice diameters and release rates were used in the experiments. The table applies to flame shape (geometry and size) as well as surface emissive power.

If experiments leave room for interpretation, Shell Global Solution prefers to calculate flame lengths slightly conservative, in order not to underestimate distances to heat radiation levels along the flame direction. Because flame

shape and surface emissive power are highly interdependent, this approach may sometimes result in a small underestimation of the surface emissive power.

Table 2 Data used for developing the Barker LPG jet fire model.

Released substance	*Number of releases used for validation*	*Range of stagnant pressures*	*Range of orifice diameters*	*Range of release rates*
propane	22 small, 89 large	6.3 to 9.7 bar(g)	3 to 52 mm	0.11 to 22 kg/s
butane	11 small, 15 large	4 to 20 bar(g)	3 to 52 mm	0.16 to 21 kg/s

More information on the validation of the model is presented in Annex 1.

2.4 Description of the Cracknell generic two-phase and liquid jet fire model as implemented in FRED

The Cracknell jet fire model is implemented in FRED for general two-phase and liquid releases of hydrocarbons. A full description of the model is given in [8]. The model is applicable to all releases of hydrocarbons, including mixtures of gaseous, two-phase and liquid hydrocarbons. A warning is issued if the discharge rate or the exit velocity is outside the validation range.

2.4.1 Qualitative description of the model

2.4.1.1 Flame shape and orientation

The flame of the Cracknell generic two-phase and liquid jet fire model consists of a tilted frustum of a cone and is displayed in Figure 3.

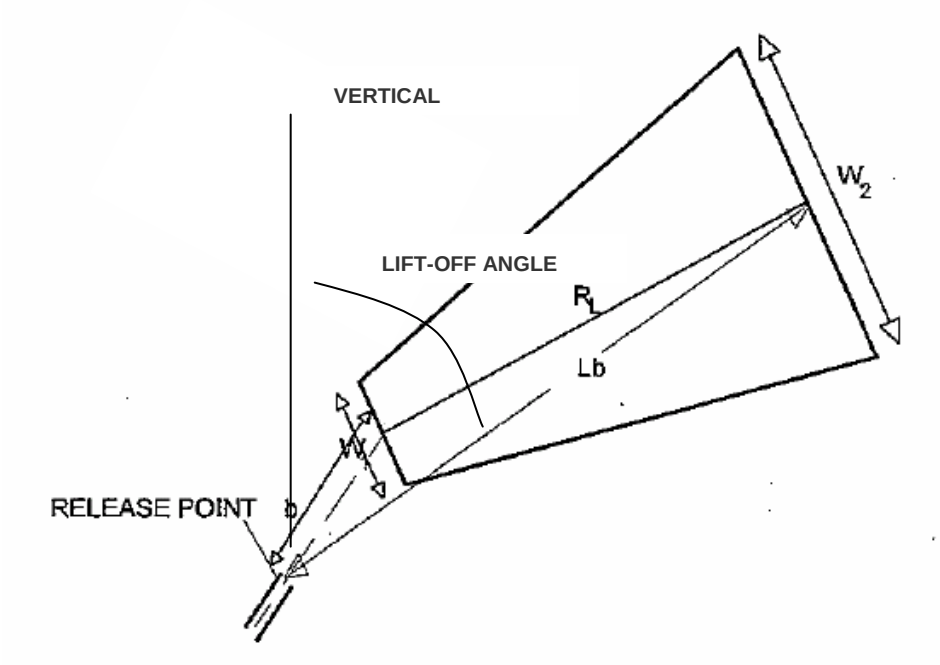

Figure 3 Flame shape for the Cracknell generic jet fire model.
Diagram obtained from Shell Global Solutions

The flame shape is characterised by the following parameters:
- flame length (L_B);
- width of the frustum base (W_1);
- width of the frustum tip (W_2);
- lift-off angle.

The flame length depends on the release rate, the heat of combustion and the velocity of the wind along the release axis. The width of the frustum base is derived from the flame length and the width of the frustum tip (with a minimum value equal to the orifice diameter). The width of the frustum tip is linear with the expanded jet diameter. A further correction is applied when the released mass contains a high fraction of non-combustible products. The lift-off angle depends on release direction and expanded jet velocity, wind direction and wind speed and buoyancy. Buoyancy is determined by flame length, expanded jet diameter and gravity.

2.4.1.2 Surface emissive power and fraction of heat radiated

In the Cracknell model, the fraction of heat radiated is derived from the release rate and the expanded jet velocity. A physical argument was used to derive a correlation between the fraction of heat radiated, mass flow and exit velocity (in particular the values of the exponents in this correlation). The missing proportionality constant was subsequently deduced from experiments. An analysis described in [8] showed that the variance in the proportionality constant was limited. A conservative value was then used for the model. The correlation does not take into consideration smoke obscuration for high release rates. Therefore, the calculated fraction of heat radiated will be more conservative for high release rates.

The surface emissive power is deduced from the total flame surface area, the total combustion power of the release and the fraction of heat radiated.

2.4.2 Validation of the model

An overview of the number of releases used for developing the Cracknell jet fire model is given in Table 3. The table also lists which orifice pressures, orifice diameters and release rates were used in the experiments. The table applies to flame shape (geometry and size) as well as surface emissive power.

Table 3 Data used for developing the Cracknell jet fire model.

Released substance	*Number of releases used for validation*	*Range of stagnant pressures*	*Range of orifice diameters*	*Range of release rates*
Butane / Natural gas	27	0.6 to 4.8 barg	40 to 80 mm	2.3 to 2.7 kg/s
Propylene	40	3.9 to 5.7 barg	3 to 6.8 mm	0.05 to 0.36 kg/s
Kerosene /natural gas	7	0.8 to 1.4 barg	80 mm	2.4 to 2.7 kg/s
Two-phase propane	22 small, 89 large	6.3 to 9.7 barg	3 to 52 mm	0.11 to 22 kg/s
Two-phase butane	11 small, 15 large	4 to 20 barg	3 to 52 mm	0.16 to 21 kg/s

If experiments leave room for interpretation, Shell Global Solution prefers to calculate flame lengths slightly conservative, in order not to underestimate

distances to heat radiation levels along the flame direction. Because flame shape and surface emissive power are highly interdependent, this attitude may sometimes result in a small underestimation of the surface emissive power.

More information on the validation of the model is presented in Annex 1.

2.5 Quantitative behaviour of the models

2.5.1 Definition of input variables

It is desirable to obtain more insight in the behaviour of the three selected models. It is not feasible however, to study every detail. Therefore, specific attention is paid to those parameters that are most relevant for the size of the consequence area of the jet fire. The following parameters were used for the model comparison:

- flame length;
- width of the frustum tip;
- fraction of heat radiated.

The consequence area depends mostly on the substance released, the pressure at the orifice (or alternatively the expanded jet velocity) and the release rate (or alternatively the orifice diameter). In this section, only releases of n-butane are discussed. Release rate and expanded jet velocity are varied.

Orifice conditions are specified as input (instead of stagnant conditions) in order to have a comparison of the jet fire models that is independent of the discharge models used. A complete overview of the assumptions and parameter choices (to be) used for the generation of the plots is given in Annex 3.

2.5.2 Results

In this subsection the quantitative behaviour of the selected jet fire models is plotted in graphs and discussed. An upper boundary of 100 kg/s is used for the discharge rate. All models are expected to be applicable in this range. In Annex 2, graphs are shown for discharge rates up to 10,000 kg/s. It is noted that the presented outcomes correspond to the inputs laid down by RIVM. The models may behave differently if other assumptions were used.

The flame length[(2)] as a function of the release rate is shown in Figure 4. Over the whole range (from 5 to 100 kg/s), the Cracknell model gives the lowest values and the JFSH-Cook model the highest. The gap between the two increases from 4%[(3)] for 5 kg/s to 11% for 100 kg/s. The predicted values by the Barker model are 4% higher than the predictions of the Cracknell model for all cases.

Figure 5 shows the flame length as a function of the expanded jet velocity for a fixed release rate of 50 kg/s. For the Barker and Cracknell models, the influence of the expanded jet velocity on the flame length is very limited. According to the JFSH-Cook model, the flame length decreases slightly with

2 In these graphs, the flame length is defined as the distance between the origin and the centre of the flame tip.

3 Difference between Cracknell and JFSH-Cook as a percentage of the lower value (Cracknell).

increasing jet velocity, yielding to a total decrease of 22% over the whole range (30 to 200 m/s).

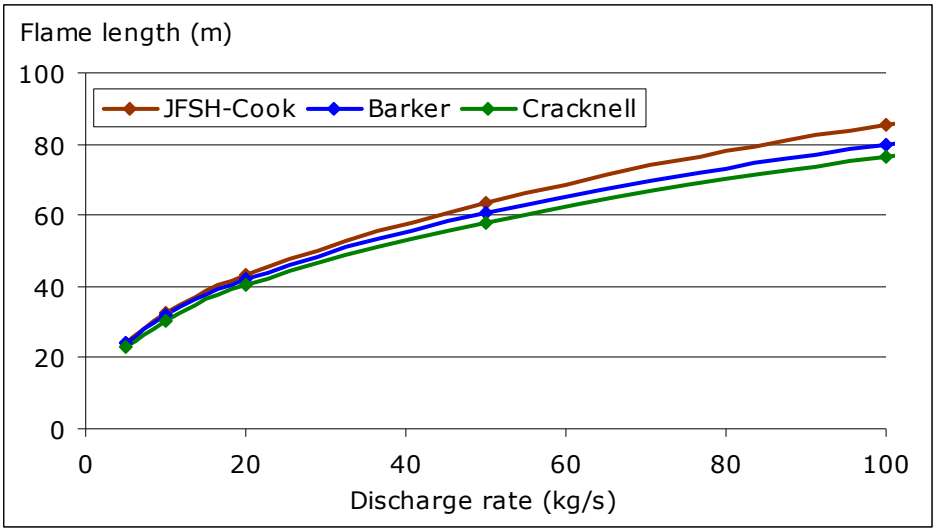

Figure 4 Flame length as a function of the release rate.

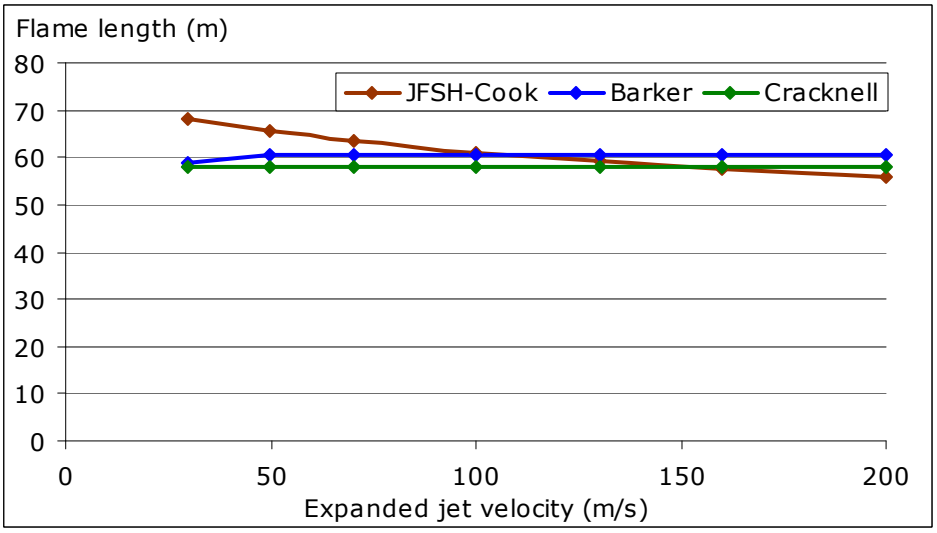

Figure 5 Flame length as a function of the expanded jet velocity (release rate 50 kg/s).

The dependence of the width of the frustum tip on the release rate is depicted in Figure 6. The Cracknell and JFSH-Cook models both show a substantial increase in tip width with increasing release rate. The Barker model shows a limited increase and has lowest predicted tip widths over the entire range (5 to 100 kg/s). For a release rate of 100 kg/s, the predictions of the Cracknell and JFSH-Cook models are roughly 100% higher than the prediction of the Barker model.

The width of the frustum tip as a function of expanded jet velocity is shown in Figure 7. According to the Barker model, the width of the frustum tip increases with increasing jet velocity. According to the Cracknell and JFSH-Cook models the tip width decreases with increasing jet velocity. The predicted values differ significantly in the lower range (Cracknell giving a four times higher value

than Barker) but tend to converge in the higher range. For 200 m/s (corresponding to a backing pressure of about 100 bar) the predicted values by both Shell models are roughly equal, and the predicted value of the DNV model is 15 to 20% higher.

It was initially expected that the flame width would be an important parameter for the flame height and therefore for the view factor near the tail of the flame. However, in the Barker and Cracknell models, the flame height depends on the flame length, the flame lift-off angle and the flame width. Therefore, a comparison of flame width alone is not very useful.

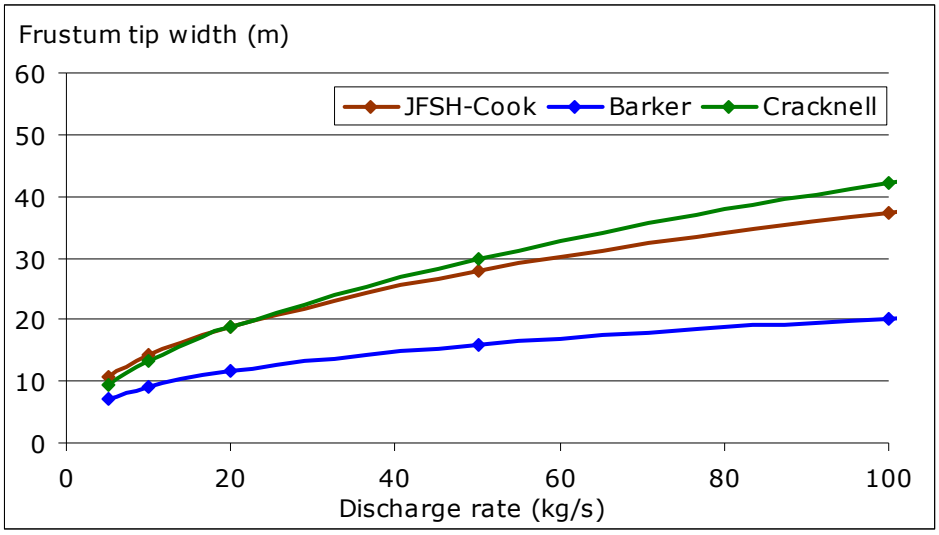

Figure 6 Width of the frustum tip as a function of the release rate.

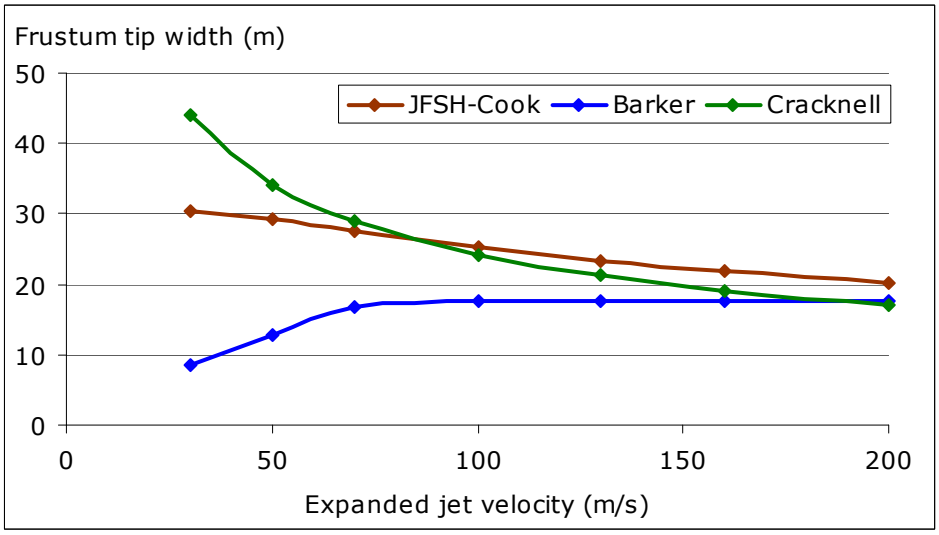

Figure 7 Width of the frustum tip as a function of the expanded jet velocity.

Figure 8 depicts the fraction of heat radiated (also known as 'emissivity') as a function of the release rate. The Barker and Cracknell models both show a decreasing emissivity with discharge rate (Barker showing the strongest decrease). The JFSH-Cook model on the other hand, predicts a constant fraction of heat radiated over the entire range (5 to 100 kg/s). For low discharge rates, JFSH-Cook predicts a fraction of heat radiated that is 26%

higher than the prediction of the Shell models. For a discharge rate of 100 kg/s, the emissivity according to the Barker model is 0.14. The emissivity according to the Cracknell model is almost 100% higher (0.27) and the emissivity according to the JFSH-Cook model 240% higher (0.47).

The fraction of heat radiated as a function of expanded jet velocity is shown in Figure 9. Again, the selected models show significantly different behaviour. The Barker model gives a constant emissivity over the entire range (30 to 200 m/s). The Cracknell model predicts a rapid decrease with increasing jet velocity and the JFSH-Cook model shows a slow decrease. The DNV model gives the highest values, being 100 to 200% higher than the values predicted by the Shell models from 50 m/s onwards.

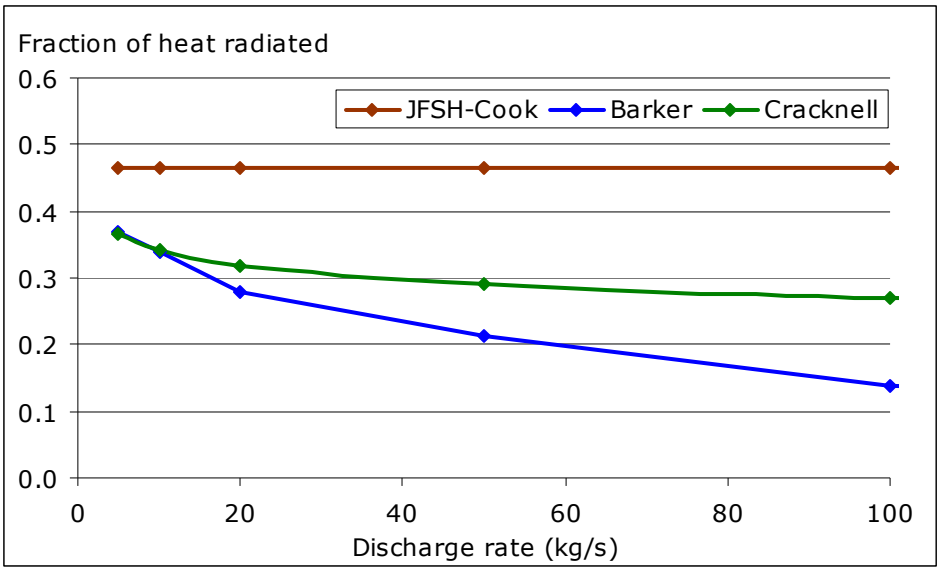

Figure 8 Fraction of heat radiated as a function of the release rate.

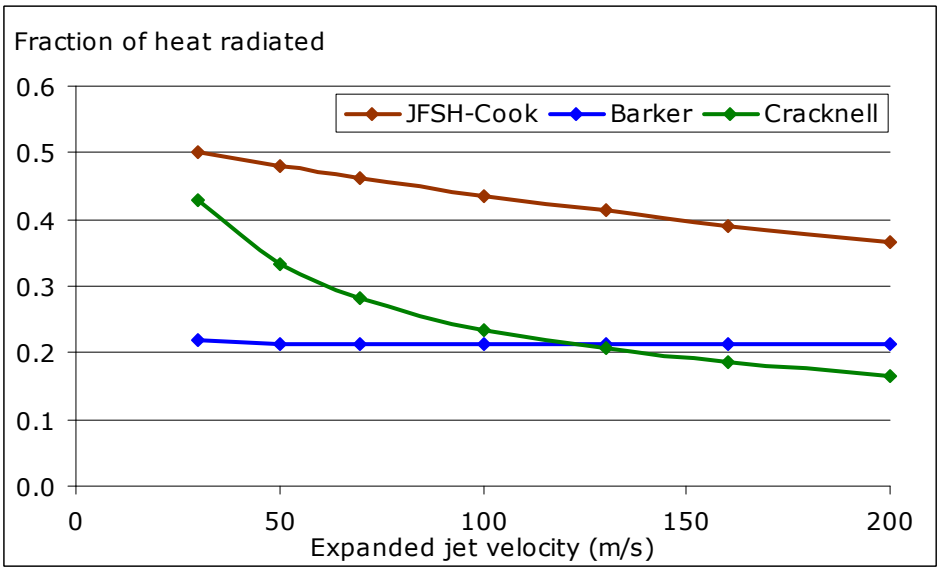

Figure 9 Fraction of heat radiated as a function of the expanded jet velocity.

2.6 Summary

The Barker model consists of a horizontal frustum of a cone and a tilted cylinder. It is therefore well suited for high pressure releases (giving a horizontal jet) with high volatility (resulting in buoyancy towards the tail). The JFSH-Cook model does not include flame lift-off and will therefore not be appropriate for highly buoyant jet fires. The Cracknell model is designed to be a generic model for two-phase and liquid hydrocarbon jet fires (both buoyant and non-buoyant). This subject will be discussed in more detail in the next two chapters.

The Barker and Cracknell models are derived from experimental outcomes for two-phase releases. The JFSH-Cook model is derived from a gaseous jet fire model. Additional assumptions are used to apply the model to two-phase and liquid releases. The amount of data used to construct the Barker and Cracknell models is significantly larger than the amount of data used to validate the JFSH-Cook model. The variance in the experimental data (such as fuels used and release conditions) is also larger for the Barker and Cracknell models in comparison with the JFSH-Cook model.

Accuracy of the models for mixtures of substances with different volatilities

The jet fire outcomes depend on discharge parameters such as discharge rate and expanded jet velocity. The jet fire model in SAFETI-NL also uses the amount of rainout. In the current text box, it is described how the discharge models in FRED and SAFETI-NL deal with multicomponent discharges.

In FRED, mixtures are treated as ideal mixtures obeying Raoult's law. In particular, mixtures are characterised by a dew point and a bubble point and the compositions of vapour and liquid are temperature dependent. It is expected that the FRED discharge models will predict the vapour and liquid fractions at the orifice well (for mixtures largely obeying Raoult's law). As a result, they will also produce reliable inputs for the jet fire models.

In SAFETI-NL, a 'pseudo-component' is used to characterise the mixture. The 'material properties' of this pseudo-component depend on the composition of the mixture. This approach is a simplification of the true behaviour of the mixture. Model outcomes may not be reliable for mixtures of substances of substantially different volatility and release conditions between the bubble point and the dew point of the mixture.

The condensates in the NAM slugcatchers have a bubble point near -160 °C and a dew point above 200 °C. These condensates contain substantial amounts of both gaseous and liquid components. As a result, the SAFETI-NL pseudo-component model is not expected to produce reliable results for these condensates. It is noted that RIVM prefers the use of pure components instead of mixtures if the composition of the mixture varies. It is further noted that a multicomponent discharge model is available in PHAST. This model is however not available for the users of SAFETI-NL.

3 Comparison of model outcomes to selected set of experimental data

3.1 Introduction

In this chapter, the Barker LPG jet fire model, the Cracknell generic two-phase and liquid jet fire model and the DNV generic two-phase and liquid jet fire model (hereafter the JFSH-Cook model) are compared to five experimental releases. Specific attention is paid to the flame shape and the surface emissive power.

3.2 Overview of the selected set of experimental data

A selection is made of five experimental horizontal two-phase or liquid releases for which sufficiently detailed information was available.

i. a release of 16.1 kg/s LPG (97% propane) with a driving pressure of 6.5 bar(g) from a 52 mm orifice, attached to a 2 m^3 vessel by a 67 m long pipeline with an internal diameter of 152 mm, as described in Davenport, Bennett, Cowley and Rowson [10] (hereafter Project AA test 3026).
ii. a release of 18.0 kg/s LPG (97% propane) with a driving pressure of 6.3 bar(g) from a 52 mm orifice, attached to a 2 m^3 vessel by a 67 m long pipeline with an internal diameter of 152 mm, as described in Davenport, Bennett, Cowley and Rowson [11] (hereafter Project AA test 3029).
iii. a release of 5.0 kg/s stabilised light crude oil with a driving pressure of 20 bar(a) from a 14 mm orifice, attached to a stationary vessel by 149 mm and 55 mm internal diameter pipework, as described in Acton, Evans and Sekulin [12] (hereafter BFETS-2 test 1).
iv. a release of 5.0 kg/s stabilised light crude oil with a driving pressure of 7.1 bar(a) from a 18 mm orifice, attached to a stationary vessel by 149 mm and 55 mm internal diameter piping, as described in Acton, Evans and Sekulin [13] (hereafter BFETS-2 test 2).
v. a release of 6.86 kg/s butane with a driving pressure of 18.85 bar(g) from a 40 mm orifice, attached to a 2 m^3 vessel by 79 m long 2 and 6 inch diameter pipework, as described in Sekulin and Acton [15] (hereafter JIVE test 8051).

Comments:

- The experiments i and ii were carried out by Shell Research in 1991, as part of the EU project 'Two-phase releases for toxic and flammable substances: thermal initiation, source term and fire effects' (also known as Project AA). It is noted that these two experiments were also included in the datasets that were used to develop the Barker and Cracknell models.
- The experiments iii and iv were performed by British Gas Research and Technology (currently GL Noble Denton) in 1996, as part of phase 2 of the project 'Blast and fire engineering for topside structures' (also known as BFETS), which was commissioned by The Steel Construction Institute. It is noted that these releases did not produce a stable flame and that a pilot flame was needed to keep the jet flame burning (as reported in [6]).
- Experiment v was carried out by British Gas in 1994, as part of the EU project 'Hazard consequences of jet-fire interactions with vessels containing pressurised liquids' (also known as JIVE).

As each of the selected jet fire models requires different inputs to remodel the selected experimental releases, only a summary of the experimental conditions is supplied (Table 4). Further information was obtained from the references. Though there is some degree of freedom in how the release conditions can be reproduced, it is vital that the release rate is in accordance with the actual release rates.

All selected releases have an angle between the release direction and the wind direction. In SAFETI-NL jet fire consequences are always calculated along the wind direction (in accordance with the Dutch QRA requirements). As the aim of this chapter is to reproduce the experimental release conditions as good as possible, the outcomes for the JFSH-Cook model are calculated with the DNV software tool PHAST because PHAST has the advantage that it offers the possibility to take into account crosswind effects. All other input data in PHAST are kept as close to SAFETI-NL as possible.

Table 4 Relevant data for selected set of experimental releases.

	Project AA test 3026	*Project AA test 3029*	*BFETS-2 test 1*	*BFETS-2 test 2*	*JIVE test 8051*
Discharge conditions					
Substance released	LPG [1]	LPG [1]	crude oil [2]	crude oil [2]	butane [3]
Tank pressure (bara)	7.53	7.34	20.0	7.1	19.85
Tank temperature (°C)	5.5	3.2	21.3 [4]	22.2 [4]	1.9
Orifice diameter (mm)	52	52	14.0	18.0	40
Discharge height (m)	3	1.5	3	3	3
Angle between release and wind direction (°) [5]	16	9	5	4	75
Release rate (kg/s)	16.1	18.0	5.0	5.0	6.86
Weather conditions					
Wind speed (m/s)	3.7	2.0	3.1	2.5	0.5
Temperature of ambient air (°C)	13.7	8.0	21.3	22.2	8.7
Relative humidity (%)	70 [6]	82	55	49	35
Atmospheric pressure (mbar)	1000	1000	992	992	995

(1) According to [5] the LPG contained 0.2 mol% ethane, 97.4 mol% propane, 1.6 mol% iso-butane, 0.8 mol% n-butane and less than 0.1 mol% propylene.

(2) The composition of the crude oil is not given in [6]. A rough estimate, based on Table 3.3 in [6] is that 2% is C6, 3% C7, 5% C8, 5% C9, 10% C11-C12, 15% C12-C15, 20% C16-C19 and 40% C20.

(3) The amount of n-butane in the commercial grade butane mix is 95.6% ([14]). For further convenience it is assumed that all butane is n-butane.

(4) The stagnant temperature is not reported. The listed value is the ambient temperature, which serves as a best estimate.

(5) Angle between the direction where the wind and release are heading. An angle of 0° implies that wind and release are heading in the same direction (enlarging the flame). An angle of 180° implies that flame and wind are opposing (causing shorter flames).

(6) RIVM erroneously prescribed 70%. The real humidity during the experiments was 59% ([10]). The error does not affect the calculated flame properties but leads to a minor underestimation of calculated distances to heat radiation levels.

3.3 Model outcomes for the selected release scenarios

The data reports for the selected releases ([10], [11], [12], [13], [15]) provide images of average flame shapes (region where flames are visible during a certain fraction of the time). In this section, these images are compared with the computed flame shapes and parameters (Barker model, Cracknell model and JFSH-Cook model).

3.3.1 Model outcomes for the selected LPG releases from Project AA

Figure 10 and Figure 11 show the results for the two LPG releases (97% propane) of project AA ([5]). Table 5 gives the corresponding numerical data. The expanded jet velocity is included in the table in order to see whether differences in outcomes are caused by true differences in the jet fire models or by differences in assumptions preceding the jet fire calculations.

As was mentioned in section 3.2, these two experiments were also used to develop the Barker and Cracknell models. As a result, the correspondence between the modelled outcomes and the measured outcomes could be higher than for a random flame. We however expect that the 'bias' is limited because the datasets that were used to construct the Barker and Cracknell models contained more than a hundred experiments and no particular weight had been given to test 3026 and test 3029.

Buoyant behaviour is visible for both jet flames (see Figure 10 and Figure 11). This buoyant behaviour is well captured by the Barker model (i.e. the Shell LPG model). The Cracknell model (i.e. the Shell generic hydrocarbon model) underestimates the buoyancy, while the JFSH-Cook model in SAFETI-NL does not take into account the buoyancy at all.

The flame length is well predicted by the Barker and Cracknell models, while JFSH-Cook overpredicts the flame length of the Project AA test 3029 release. The total flame surface area appears to be overestimated by all three models (mostly by JFSH-Cook).

The fraction of heat radiated is 0.35 according to the JFSH-Cook model (average for both releases), 0.26 according to the Barker model and 0.31 according to the Cracknell model. Unfortunately, the total amount of heat radiated is not reported in the data reports. All calculated mean surface emissive powers are substantially lower than the measured surface emissive powers. A possible explanation is that the selected models try to predict the total amount of heat radiated correctly. If the total flame surface area is overpredicted, the mean surface emissive power will be lower than experimentally observed.

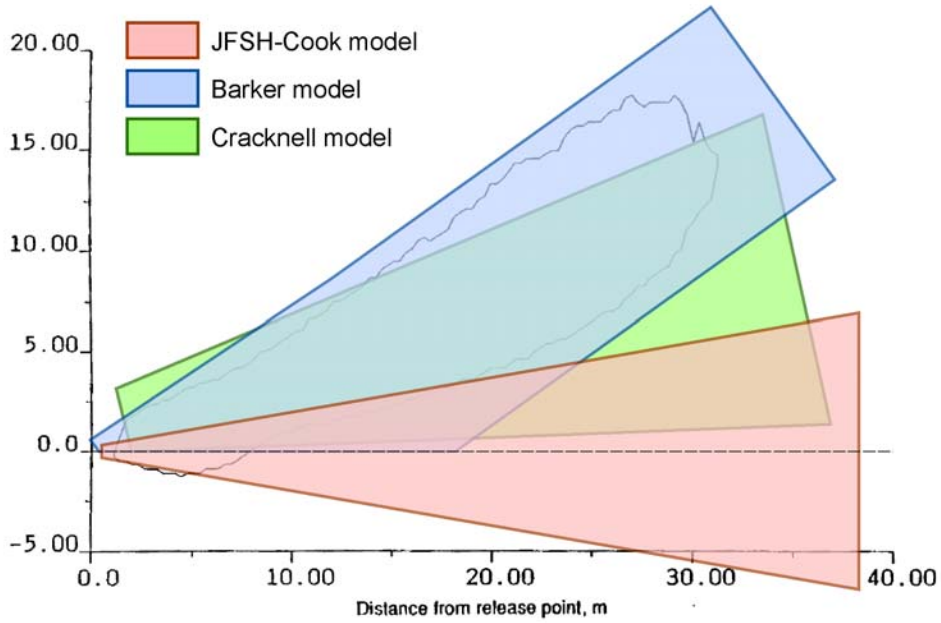

Figure 10 Measured flame shape (50% flame occurrence) for Project AA test 3026 compared to model outcomes.
Flame occurrence diagram taken from [10].

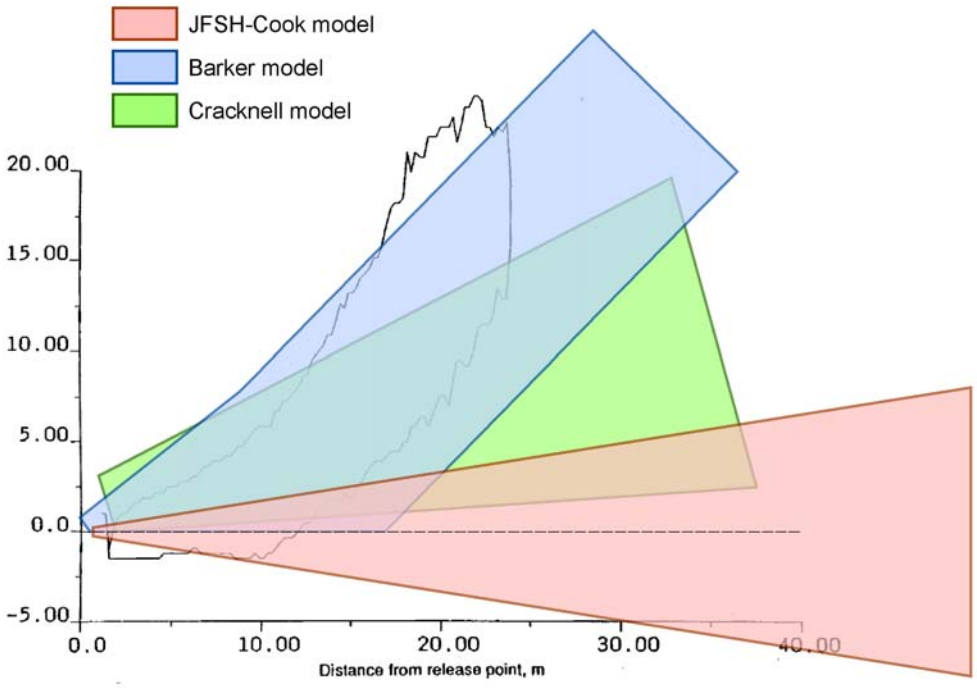

Figure 11 Measured flame shape (50% flame occurrence) for Project AA test 3029 compared to model outcomes.
Flame occurrence diagram taken from [11].

Table 5 Model outcomes for Project AA test 3026 and 3029.

	Measured outcome	*JFSH-Cook model*	*Barker model*	*Cracknell model*
Project AA test 3026				
Substance used in calculations	not applicable	propane	LPG [2]	LPG [3]
Mass involved in jet (kg/s)		16.1	16.1	16.1
Expanded jet velocity (m/s)	not reported	153	79	76
Flame length (m) [1]	31.1 [4]	38.3	37.7	34.3
Flame width at tip (m)	not reported	13.8	10.6	15.8
Flame lift off angle (°)	not reported	0	36	12
Surface emiss. power (kW/m^2)	331 [5]	253	231	178
Fraction of heat radiated	not reported	0.35	0.27	0.30
Distance to 35 kW/m^2 (m)	not reported	54 [6]	37 [6]	44 [6]
Distance to 9.8 kW/m^2 (m)	not reported	69 [6]	56 [6]	60 [6]
Project AA test 3029				
Substance used in calculations	not applicable	propane	LPG [2]	LPG [3]
Mass involved in jet (kg/s)		18.0	18.0	18.0
Expanded jet velocity (m/s)	not reported	146	69	76
Flame length (m) [1]	30.7 [7]	49.4	39.4	34.9
Flame width at tip (m)	not reported	16.0	11.2	17.8
Flame lift off angle (°)	not reported	0	46	15
Surface emiss. power (kW/m^2)	294 [5]	197	231	182
Fraction of heat radiated	not reported	0.35	0.26	0.32
Distance to 35 kW/m^2 (m)	not reported	65	36	46
Distance to 9.8 kW/m^2 (m)	not reported	80	57	65

(1) The reported lengths are measured along the flame direction. The flame direction may deviate from the release and wind directions.

(2) The LPG mix used contains 97.4% propane and 2.6% butane.

(3) A mix of common LPG components is defined, containing 97.3 mol% propane.

(4) The reported experimental flame length is derived from the best fit of a frustum of a cone and a cylinder with the 50% occurrence flame diagram (sum of cone top boundary length and cylinder length, see Figure 2 for further explanation).

(5) Mean flame surface emissive power (averaged over a time period of 10 to 15 seconds).

(6) By mistake, a value of 70% was prescribed for the humidity (it should have been 59%). As the absorption of radiation in air increases with humidity, the distances to 35 and 9.8 kW/m2 are slightly underestimated.

(7) A value of 25.9 m was reported in [11], but this value is expected to be erroneous. The value of 30.7 m is taken from an internal document from Shell Global Solutions and is well in line with the flame occurrence diagram (see Figure 11).

3.3.2 Model outcomes for the selected crude oil releases from BFETS (phase 2)

Figure 12 and Figure 13 show the results for two crude oil releases of phase 2 of the BFETS project ([6]). Table 6 gives the corresponding numerical data. As noted at the start of this section, the crude oil only releases in BFETS phase 2 did not produce stable flames and needed pilot flames to keep the jet flame burning. It should further be noted that the Barker model is designed for LPG jet fires (and not for crude oil). The outcomes of the Barker model are only included in this subsection for reasons of comparison.

Figure 12 and Figure 13 show that the selected crude oil jet are less buoyant than the LPG jets presented in the previous subsection. In test 1 (Figure 12) the flame has lifted roughly 4 meters at a downwind distance of 25 m. In test 2 (Figure 13), the jet flame remained horizontal. A possible explanation is that a large part of the crude oil remains liquid, thereby increasing the density of the jet and reducing the buoyancy. The evaporation of droplets also reduces the temperature of the jet and thereby buoyancy.

Considering flame length, the selected models seem to underpredict for test 1 and overpredict for test 2. On the average, the JFSH-Cook model and the Cracknell model are in the right order of magnitude, while the flame length from the Barker model is slightly higher than the measured value. The total flame surface area is overestimated by both Shell models for test 2.

Considering flame lift-off, no pronounced conclusions can be drawn from test 1. The flames from the Barker and Cracknell models seem to cover the measured flame better, but the JFSH-Cook model is more aligned with the core of the flame (high occurrence percentage). For test 2, the two Shell models calculated substantial lift-off whereas the real flame remains horizontal. The JFSH-Cook model produces a good resemblance of the flame for this test.

The fraction of heat radiated (average for test 1 and test 2) is 0.48 according to the JFSH-Cook model, 0.37 according to the Barker model and 0.39 according to the Cracknell model. The average fraction of heat radiated for the pure crude oil releases in BFETS - phase 2 was 0.40 (personal correspondence with GL Noble Denton).

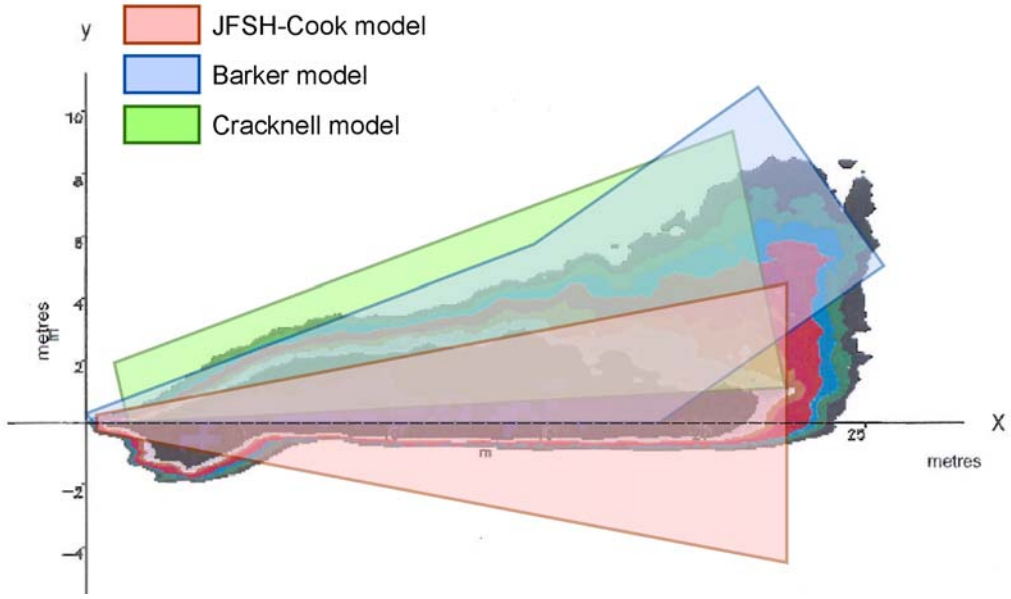

Figure 12 Measured flame shape for BFETS-2 test 1 compared to model outcomes (the zone between blue and red refers to 50% flame occurrence).

Flame occurrence diagram taken from [12].

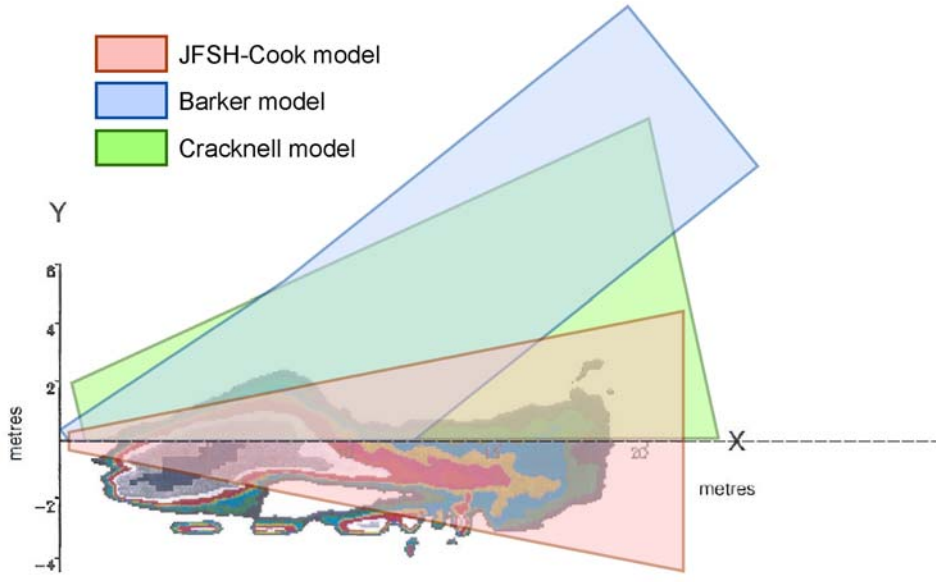

Figure 13 Measured flame shape for BFETS-2 test 2 compared to model outcomes (the orange/yellow zone between blue and red refers to 50% flame occurrence).

Flame occurrence diagram taken from [13].

Table 6 Model outcomes for BFETS-2 test 1 and test 2.

	Measured outcome	*JFSH-Cook model*	*Barker model* [2]	*Cracknell model*
BFETS-2 test 1				
Substance used in calculations	not applicable	n-nonane	butane	crude mix [3]
Mass involved in jet (kg/s)		5.00	5.00	5.00
Expanded jet velocity (m/s)	not reported	75	81	82
Flame length (m) [1]	26 [4]	22.5	24.1	20.9
Flame width at tip (m)	not reported	9.0	7.0	8.4
Flame lift off angle (°)	not reported	0	35	12
Surface emiss. power (kW/m^2)	287 [5]	258	255	178
Fraction of heat radiated	not reported	0.46	0.37	0.33
Distance to 35 kW/m^2 (m)	not reported	33	28	25
Distance to 9.8 kW/m^2 (m)	not reported	42	39	35
BFETS-2 test 2				
Substance used in calculations	not applicable	n-nonane	butane	crude mix [3]
Mass involved in jet (kg/s)		3.3 [6]	5.00	5.00
Expanded jet velocity (m/s)	not reported	46	46	46
Flame length (m) [1]	23 [4]	21,2	24.1	21.1
Flame width at tip (m)	not reported	8.9	7.0	11.1
Flame lift off angle (°)	not reported	0	39	12
Surface emiss. power (kW/m^2)	203 [5]	187	255	176
Fraction of heat radiated	not reported	0.49	0.37	0.44
Distance to 35 kW/m^2 (m)	not reported	29	23	27
Distance to 9.8 kW/m^2 (m)	not reported	38	36	39

(1) The reported lengths are measured along the flame direction. The flame direction may deviate from the release and wind directions.

(2) As discussed in the plain text, the Barker model is not designed for modelling crude oil jet fires. It is added solely for reasons of comparison.

(3) The mix of paraffins used contained 2 mol% n-hexane, 3% n-heptane, 5% n-octane, 5% n-nonane and 85% n-decane.

(4) According to [12] and [13], the reported flame length corresponds to the time-averaged horizontal length of the visible flame. The reported flame lengths are a little larger than the furthest distances from the orifice to the 20% occurrence contours in Figure 12 and Figure 13. According to personal correspondence with Advantica (formerly British Gas Research), the discrepancy is caused by parts of the burning flame near the tail that are obscured by soot most of the time, and therefore are not visible in the 20% occurrence diagram.

(5) The maximum surface emissive power at any location within the visible flame as reported in [12] and [13]. This value is fundamentally different from the average surface emissive power calculated by the jet fire models.

(6) The mass involved in the jet fire (3.3 kg/s) is smaller than the release rate (5.0 kg/s) because SAFETI-NL predicts a considerable rainout for this scenario (78.2%). See also section 2.2.1.

3.3.3 *Model outcomes for the selected butane release from JIVE*

Figure 14 shows the results for the butane releases of the JIVE project ([14]). Table 7 gives the corresponding numerical data.

The butane jet fire clearly shows buoyant behaviour. The centre of the tail is about 6 m higher than the orifice position. The Cracknell model shows a very good match for the flame lift-off. The Barker model overestimates the buoyancy, while the JFSH-Cook model does not include buoyancy.

Flame length and total flame surface area are overpredicted by all three models. JFSH-Cook performs worst, with an estimated flame length of 36 m (twice as much as the real flame length). The Barker model overestimates the flame length by nearly 50%, the Cracknell model 30%.

The fraction of heat radiated is 0.50 according to the JFSH-Cook model, 0.36 according to the Barker model and 0.54 according to the Cracknell model. Unfortunately, the total amount of heat radiated is not reported in the data report.

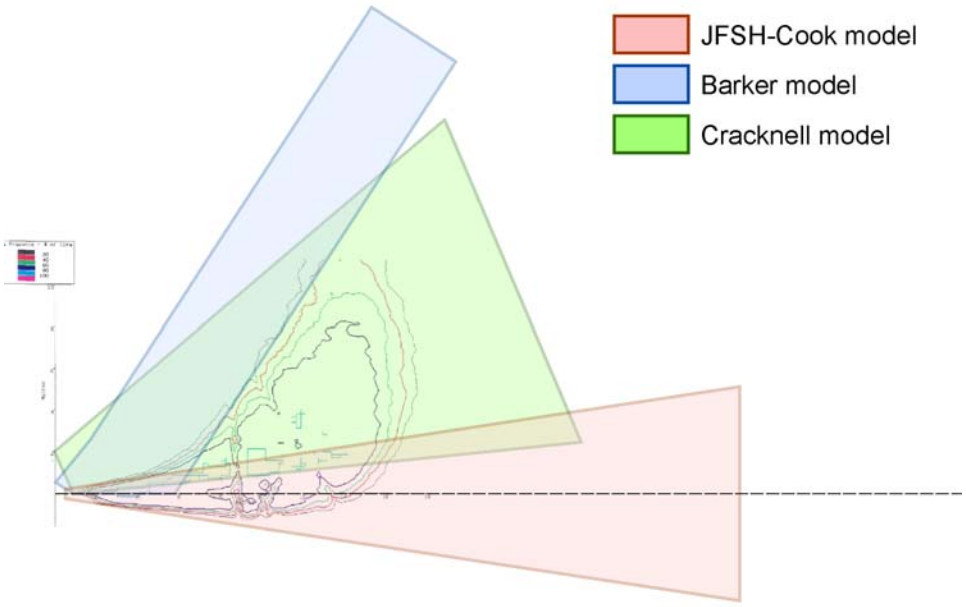

Figure 14 Measured flame shape for JIVE test 8051 compared to model outcomes (the red line marks 40% flame occurrence, light blue 60% flame occurrence).
Flame occurrence diagram taken from [15].

Table 7 Model outcomes for JIVE test 8051.

	Measured outcome	*JFSH-Cook model*	*Barker model*	*Cracknell model*
JIVE test 8051				
Substance used in calculations	not applicable	n-butane	butane	butane
Mass involved in jet (kg/s)		6.86	6.86	6.86
Expanded jet velocity (m/s)	not reported	9.3	15	28
Flame length (m) (1)	18.3 m (2)	32.8	27.4	23.4
Flame width at tip (m)	not reported	10.27	4.8	16.8
Flame lift off angle (°)	not reported	0	57	23
Surface emiss. power (kW/m^2)	(3)	240	255	175
Fraction of heat radiated	not reported	0.48	0.36	0.54
Distance to 35 kW/m^2 (m)	not reported	44	16.7	30.2
Distance to 9.8 kW/m^2 (m)	not reported	56	36.1	48.5

(1) The reported lengths are measured along the flame direction. The flame direction may deviate from the release and wind directions.

(2) Distance from the orifice to the 20% flame occurrence tail at 6 m height, derived from Figure 20 in [15]. The maximum horizontal distance to 50% flame occurrence is roughly 16.6 m.

(3) Only the spot surface emissive power for two locations is reported in [15]. It was not deemed appropriate to compare spot surface emissive powers with average surface emissive powers.

3.4 Discussion of outcomes

In the previous section, outcomes of five experimental releases were compared to predictions from the JFSH-Cook model, the Barker model and the Cracknell model. In the current section the main findings are summarised and compared to additional information found in the literature. Flame size, flame shape and flame orientation (direction) are discussed first and subsequently the amount of heat radiated by the flame will be analysed.

It is noted that the jet fire models are designed to be 'cautiously realistic'. In order not to underestimate consequence distances along the flame direction, the flame length is calculated slightly conservative. The total amount of heat radiated is predicted as accurate as possible. As a result, the flame surface emissive power may sometimes be underestimated. A good reason to apply some conservatism in the calculation of flame length is that the radiant flame is usually bigger than the visible flame (see Figure 15). A large amount of black smoke is often seen towards the tail of the flame, which obscures the burning flame and is sufficiently warm to emit heat radiation.

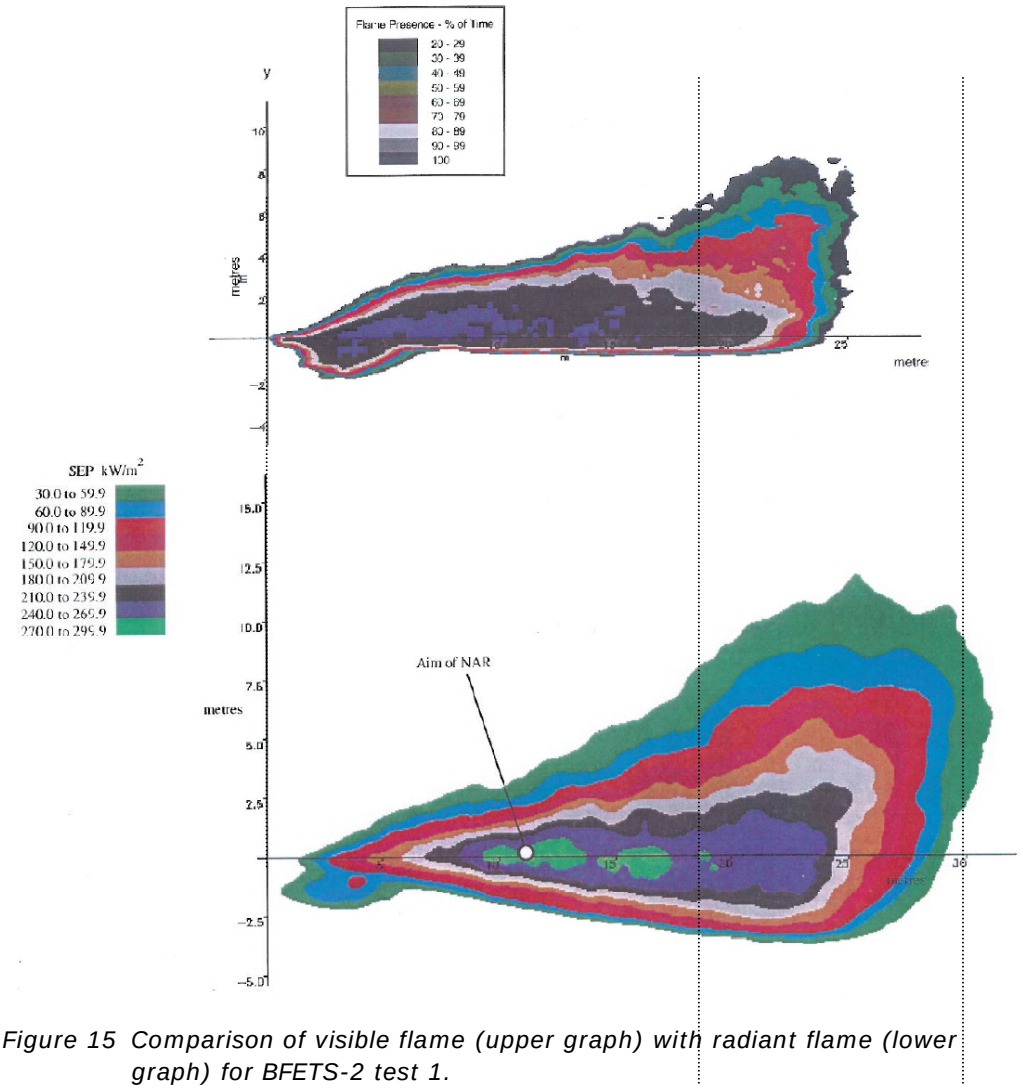

Figure 15 Comparison of visible flame (upper graph) with radiant flame (lower graph) for BFETS-2 test 1.

Pictures obtained from [12].

Flame occurrence increases from 20% (grey) to 100% (purple). Surface emissive power increases from 30 kW/m2 (dull green) to 300 kW/m2 (bright green).

3.4.1 Flame size, flame shape and flame orientation

The results from sections 3.3.1, 3.3.2 and 3.3.3 were used for a qualitative judgement of the 'goodness of fit' between the predicted flame shapes and the measured (average) flame shapes. The various figures in sections 3.3.1, 3.3.2 and 3.3.3 were inspected visually and an assessment was made if the match between prediction and measurement was 'good', 'reasonable' or 'not good'. The results are shown in Table 8. No distinct criteria were used, but it is expected that a more transparent assessment would produce similar results.

Table 8 shows that the Cracknell model performs reasonable to good for all five selected releases. The Barker model performs well for the propane releases of project AA but overestimates buoyancy and flame surface area for BFETS-2 test 2 (crude oil) and buoyancy for JIVE test 8051 (butane). JFSH-Cook performs well for the crude oil releases of BFETS, but underestimates the

flame lift-off of the propane and butane releases. JFSH-Cook also overpredicts the flame length (flame surface area) for JIVE test 8051 (butane).

Table 8 Qualitative assessment of the goodness of fit of the selected models with respect to flame shape, size and orientation.

Release	*JFSH-Cook model*	*Barker model*	*Cracknell model*
Project AA test 3026	reasonable	good	good
Project AA test 3029	poor	good	reasonable
BFETS-2 test 1	good	good (1)	good
BFETS-2 test 2	good	poor (1)	reasonable
JIVE test 8051	poor	reasonable	reasonable

(1) It is noted that the Barker model is not intended to be used for crude oil jet fires.

A conclusion that can be drawn from Table 8 is that, with respect to flame shape, size and orientation, the Cracknell model is a better generic model than the JFSH-Cook model. The Barker model should by design do well for propane and butane releases, and indeed gives good results for project AA. The JFSH-Cook model does not include flame lift-off and performs best for releases of non-volatile liquids.

3.4.2 Fraction and amount of heat radiated

The amount of heat that is radiated is one of the key parameters of a jet fire model because the amount of heat received is linear with the amount of heat radiated. The amount of heat that is radiated is the product of the fraction of heat radiated (also referred to as *F*-value) and the total heat produced. An overview of the predicted *F*-values for the selected experimental releases is given in Table 9. The table shows that the Barker model gives relatively low *F*-values (between 0.26 and 0.37), whereas the JFSH-Cook model predicts relatively high *F*-values (between 0.35 and 0.49). For each release, the maximum value is 30% to 50% higher than the minimum value.

The amount or fraction of heat radiated in the selected experiments was not reported in the corresponding data reports ([10], [11], [12], [13] and [15]). Only average surface emissive power, maximum spot surface emissive power and arbitrary spot surface emissive power were reported, but these values are of limited use for the current analysis. Therefore, the fraction of heat radiated will be estimated from the information available in the public literature.

Various literature sources are available on the physical mechanisms for heat radiation from flames (e.g. [16], [17]). The energy that is produced in a flame is transformed into convective energy (heating of combustion products and entrained air) and heat radiation. The heat radiation is predominantly produced by soot in the flame. Soot is both a good emitter and a good absorber of heat radiation and the influence of the soot depends on the amount of soot.

- [Optically thin flame] In the optically thin regime, an increase of soot yields to more radiation production while the absorption of heat radiation remains low. In this regime, a larger amount of soot results in a higher amount of heat radiation received by an observer outside the flame.
- [Optically thick flame] In the optically thick regime, soot in the outer regions of the flame absorbs the radiation produced in the inner regions of the flame. In other words, the inner region of the flame is shielded (or obscured). As a consequence, only the radiation produced in the outer

regions of the flame is relevant for observers outside the flame. In this regime, the received heat radiation depends on the size of the flame and is not very sensitive to the specific amount of soot.

The amount of soot in the flame is determined by the type of fuel and the quality of the mixing with air. Fuels with higher carbon numbers (e.g. condensates) produce more soot than fuels with low carbon number (in particular methane). Good mixing reduces the amount of soot. Release rate and jet velocity are the most important parameters for the quality of the mixing.

In Guigard, Kindzierski and Harper ([17]) a literature survey was carried out for the fraction of heat released from flares and various observational data are presented. Several of their references illustrate that the *F*-value is highly dependent on jet velocity. For propane, the fraction diminishes from about 0.37 for 0 m/s exit velocity to 0.15 for an exit velocity of 60 m/s (originally reported in [18], graph reproduced in Figure 16). Similar behaviour was found by these and other authors for methane. Guigard, Kindzierski and Harper also discussed the influence of wind speed and wind direction and noted that no significant correlation between *F*-values and wind conditions was found by Cook, Fairweather, Hammonds and Hughes ([19]).

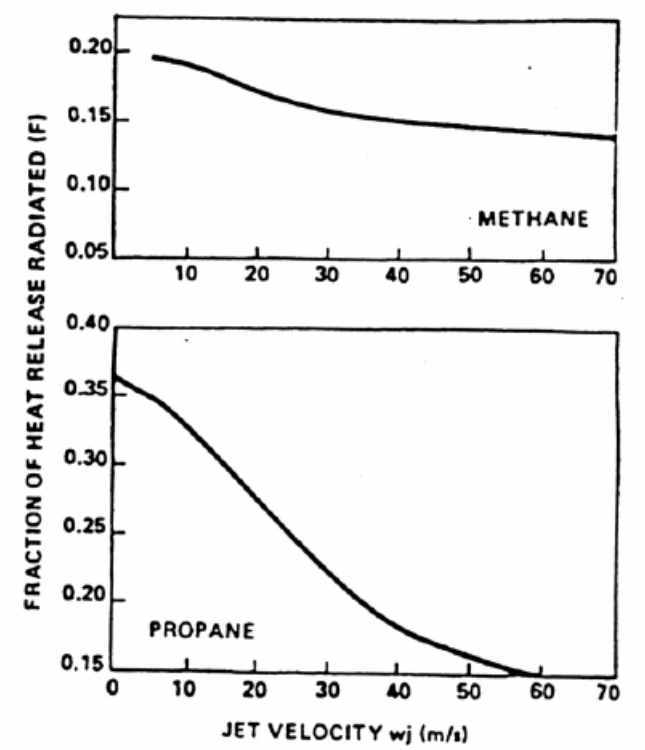

Figure 16 Fraction of heat radiated as a function of expanded jet velocity.
Reproduced from [18]

In Lowesmith, Hankinson, Acton and Chamberlain ([20]), observational data of some 170 experiments are presented in a plot. An average *F*-value of 0.13 is proposed for methane releases, 0.24 for propane, 0.32 for butane and 0.5 for crude oil. If the data points in the plot are studied in more detail, it can be seen that the *F*-value varies between (roughly) 0.06 and 0.34 for methane, 0.17 and 0.43 for propane, 0.13 and 0.48 for butane and 0.37 and 0.67 for

crude oil. This is in line with the observations made in [17]. The upper end of the validation of the data in [20] is 18 kg/s for propane, 29 kg/s for butane and 16 kg/s for crude oil.

Based on the above, the following conclusions are drawn with respect to the selected experiments (see also Table 9):

- Project AA test 3026 and 3029: according to literature, the *F*-value for propane can be somewhere between 0.15 and 0.45 with an average value of 0.24. Considering the relatively high exit velocities of 70 m/s or more in the selected releases, this average value of 0.24 is expected to be conservative (e.g. see Figure 16). The Barker model then produces the best results whereas the Cracknell model and (particularly) the JFSH-Cook model are overconservative.
- BFETS-2 test 1 and test 2: according to personal correspondence with Mike Acton (GL Noble Denton, formerly British Gas Research), the *F*-value for the pure crude oil releases in BFETS phase 2 was about 0.4 (the statement that it was below 0.3, as reported in [21], is incorrect). It is concluded that the Barker and Cracknell models give fairly accurate results and the JFSH-Cook model gives slightly conservative results.
- JIVE test 8051: according to literature, the *F*-value for butane can be somewhere between 0.15 and 0.50 with an average value of 0.32. The expanded exit velocity does not appear to be either high or low. Test 8051 was part of the JIVE project, and the *F*-value for various of these releases was plotted in Figure 4 of Lowesmith et al. The value 0.32 appears to be the best guess for test 8051 (which – unfortunately – is not reported in the above-mentioned figure). In that case, the Barker model (again) gives the most accurate prediction while the Cracknell and JFSH-Cook models overestimate the amount of heat produced.

Table 9 Summary data for the fraction of heat radiated.

Release	*JFSH-Cook model*	*Barker model*	*Cracknell model*	*RIVM estimate*
Project AA test 3026	0.35	0.27	0.30	0.24
Project AA test 3029	0.35	0.26	0.32	0.24
BFETS-2 test 1	0.46 (1)	0.37 (2)	0.33	0.4
BFETS-2 test 2	0.49 (1)	0.37 (2)	0.44	0.4
JIVE test 8051	0.48	0.36	0.54	0.32

(1) Outcome based on n-nonane instead of crude oil.

(2) Outcome based on n-butane instead of crude oil.

Overall the outcomes of the Barker model are deemed most reliable, with deviations from the expected values ranging from -7% to +13%. This is somewhat surprising because the influence of release rate and exit velocity is not incorporated in the Barker model. The Cracknell model has larger deviations from the expected value (ranging from -17% to +69%), and appears to be slightly conservative on the average (24% average overprediction). The JFSH-Cook is conservative for all cases (ranging from +15% to +56%) with an average overprediction of 36%. It is noted however that the uncertainty in *F*-values is considerable, foremost because reliable data on the *F*-value of butane and higher hydrocarbons are sparse.

3.5 Summary and conclusions

In this chapter the three selected jet fire models were compared to a set of five experimental releases. The measured flame shapes were compared to predicted flame shapes in five separate visual images. Other outcomes were compared in tabular form.

With respect to the flame size, flame shape and flame orientation, it was concluded that the Cracknell model is the best generic model. The Barker model may produce better results for volatile liquids (such as propane) and the JFSH-Cook model may produce better results for non-volatile releases.

The uncertainty in the fraction of heat radiated is substantial. Based on several statements made in the literature it is expected that the Barker model gives the most accurate results for the selected set of experiments. The Cracknell model is on the conservative side and the JFSH-Cook model appears to be more conservative.

4 Extrapolation of the models

4.1 Introduction

In the previous chapter a comparison was carried out of model outcomes for measured flame data. In the current chapter model outcomes for the NAM Den Helder QRA scenarios will be compared. This is relevant because the input data for these scenarios are well outside the validation range of all three selected jet fire models. The aim of this chapter is to find out whether the behaviour of the models can still be regarded as plausible when applied to the NAM Den Helder cases. The assessment to which extent the model outcomes are plausible is supported by a study of various dispersion outcomes and a literature study.

Further insight in extrapolation of the different models is provided in Annex 2.

4.2 Extrapolation to the NAM Den Helder QRA scenarios

The NAM Den Helder site is a location where three gas pipelines from North Sea gas production platforms come ashore. Each of these incoming pipelines is connected to a pipe manifold which divides the incoming gas and condensate over a set of parallel pipes. These downstream pipes have a small inclination (declination). Gas leaves the pipes at the top and condensate leaves the pipes at the bottom. The combination of pipe manifold and attached parallel pipes is labelled a 'slugcatcher'. The three systems are referred to as 'Nogat', 'Hical' and 'Local'.

In 2007 it was proposed that the following release scenarios should be used for each slugcatcher:

- full bore rupture of one of the pipes with a release from the vapour space;
- leak from one of the pipes with a release from the vapour space;
- full bore rupture of one of the pipes with a release from the liquid space;
- leak from one of the pipes with a release from the liquid space.

According to Dutch prescriptions for third party risk calculation ([22]), these releases have to be modelled as horizontal releases along the wind direction. As the pipelines of the slugcatchers are interconnected at both top and bottom and as a whole connected to pipelines upstream and downstream, the release rate in case of a rupture of a pipe is not easily calculated. In 2007 the release rates of Table 10 were proposed. The calculated consequence distances corresponding to the release rates of Table 11 are considerable, and indeed the full bore rupture scenarios turned out to be dominant for the location of the IR 10^{-6} contour of the NAM Den Helder site.

The scenarios in Table 10 for Nogat, Hical and Local all involve large diameter pipes at high pressure. Therefore, only the outcomes for the Hical release scenario will be investigated in detail. It is expected that the model outcomes for Nogat and Local will show similar patterns.

Table 10 Description of the full bore rupture QRA scenarios for NAM Den Helder.

Slugcatcher	**Local**	**Hical**	**Nogat**
Substance	Local	Hical	Nogat
Pressure	40 bar (abs.)	70 bar (abs.)	88 bar (abs.)
Temperature	5 °C	5 °C	5 °C
Internal diameter	1.176 m	0.876 m	1.176 m
Length	2×238 m	8×238 m	4×215 m
Release from vapour space			
Initial release rate (4)	5000 kg/s	5000 kg/s	12,000 kg/s
Release rate: average 0 - 20 s (4)	1836 kg/s	3280 kg/s	5225 kg/s
Release from liquid space			
Initial release rate (5)	16,000 kg/s	16,000 kg/s	33,500 kg/s
Release rate: average 0 - 20 s (5)	5310 kg/s	9483 kg/s	13,332 kg/s

(1) The Local natural gas condensate mixture consists of 1.6 wgt% methane, 0.3% ethane, 0.2% propane, 0.3% butane, 0.4% pentane, 1% hexane, 5.1% heptane, 10.3% octane, 69.8% nonane, 10.4% benzene and 0.1% inert gases.

(2) The Hical natural gas condensate mixture consists of 5.5 wgt% methane, 2.5% ethane, 2.4% propane, 2.9% butane, 3.3% pentane, 6.2% hexane, 10.3% heptane, 12% octane, 41.4% nonane, 12.9% benzene and 0.1% inert gases.

(3) The Nogat natural gas condensate mixture consists of 7.9 wgt% methane, 3.8% ethane, 4.6% propane, 5.6% butane, 5.6% pentane, 8.1% hexane, 8.3% heptane, 6.2% octane, 38.1% nonane, 11.2% benzene and 0.1% inert gases.

(4) Outcome of CFD-calculation carried out by SGS

(5) Outcome of CFD-calculation carried out by SGS

The required input data for the Hical scenario are listed in Table 11. Expanded jet conditions are specified as input instead of stagnant conditions in order to have a comparison of the jet fire models that is independent of the discharge models used. As the selected models differ, a distinction is made between essential input data (required) and input data that needs to be approximated as good as possible.

It is noted that these input data are considerably outside the validation range of each of the selected jet fire models. It is further noted that the Barker model is not designed for releases of gas condensate. Results are displayed solely for reasons of comparison.

Table 11 Input data for the selected NAM Den Helder QRA scenario.

Essential input data	
Substance released	Hical
Release rate	9483 kg/s (1)
Orifice diameter	876 mm
Jet velocity after expansion	46.33 m/s
Vapour (mass) fraction after expansion	0.03
Release height	5 m
Release direction	horizontal, along wind
Wind speed	5 m/s
Temperature of ambient air	8 °C
Humidity	86.3%
Atmospheric pressure	101550 Pa
Stability of atmosphere	Pasquill Gifford Class D

Table 11 (continued)

Further input data to be approximated as good as possible	
Stagnant pressure	5.07 bar (g)
Stagnant temperature	5 °C
Liquid head above orifice	5 m
Final temperature	-0.5 °C

(1) The chosen release rate is a time-average over the first 20 s of the supposed rupture.

The model outcomes are given in Table 12. The flame shape according to the different models is depicted in Figure 17. The JFSH-Cook model gives the biggest flame (both biggest length and biggest width) and is by definition entirely horizontal. The Barker model gives the smallest flame and has considerable lift-off (based on the assumption that butane is released). The Cracknell model is in between, both in flame size and in flame lift-off. The JFSH-Cook model also predicts the highest amount of heat radiated (0.31). The Barker and Cracknell models predict significantly lower values (0.12 and 0.095 respectively).

Table 12 Model outcomes for the selected NAM Den Helder QRA scenario.

	JFSH-Cook model (1)	*Barker model* (2)	*Cracknell model* (3)
Flame length (m)	579	494	410
Flame width at tip (m)	260	58	226
Flame lift off angle (°)	0	50	21
Surface emissive power (kW/m^2)	400	255	183
Fraction of heat radiated	0.31	0.12	0.095
Distance to 35 kW/m^2 (m)	890	360	520
Distance to 9.8 kW/m^2 (m)	1180	660	742

(1) Several problems were encountered when modelling this QRA scenario in PHAST using a (pseudo)mixture. In order to obtain robust results, it was decided to model the release with n-butane instead of Hical.

(2) As the Barker model can only model releases of propane, butane and mixtures of both, the outcomes are based on a release of pure n-butane (considered to be most representative for the 'Hical mixture').

(3) For efficiency reasons, pre-existing outcomes based on a release of Nogat were used. The fraction of volatile components is slightly higher in Nogat than in Hical. The differences in outcomes are expected to be very limited.

The Barker model gives the shortest consequence distances. This is a result of the small flame size, the significant flame lift-off and a low fraction of heat radiated (*F*-value). The Cracknell model predicts a total heat radiation that is 20% lower than that of the Barker model, but due to the different flame position, the consequence distances are higher. The consequence distances of the JFSH-Cook model are highest, primarily as a result of the large amount of radiated heat that is predicted (200% higher than the Cracknell model), and secondary because the high flame length and low (no) flame lift-off.

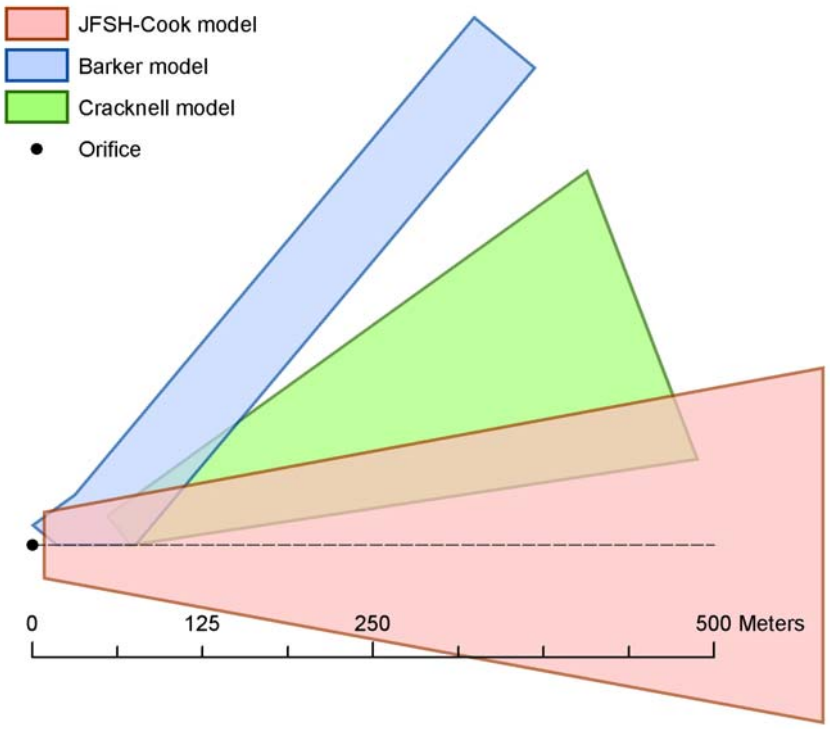

Figure 17 Comparison of calculated flame shapes for the selected NAM Den Helder QRA scenario.

4.3 Discussion of the applicability of the models for the Den Helder QRA scenarios

In the previous section, model outcomes were presented for one of the prescribed QRA scenarios for the NAM Den Helder site. The scenario involved a horizontal release of 9483 kg/s natural gas condensate. This release rate is significantly higher than the release rates that were used for the construction and validation of jet fire models (up to 18 to 22 kg/s, see chapter 2). Of further interest is that the released substance is a mixture of hydrocarbons and not a pure component. In this section it is therefore discussed to which extent the calculated model outcomes for the QRA scenario are reliable. Specific attention is paid to flame length, flame lift-off (buoyancy) and amount of heat radiation.

4.3.1 Flame length

Figure 18 shows the predicted flame length in the extrapolated range. Butane was used as release substance. Further details on the input values are provided in Annex 3. At low release rates, the predicted flame lengths are almost equal. For higher release rates, the outcomes of the Barker and Cracknell models are comparable while the flame length predicted by the JFSH-Cook model is 10 to 20% larger.

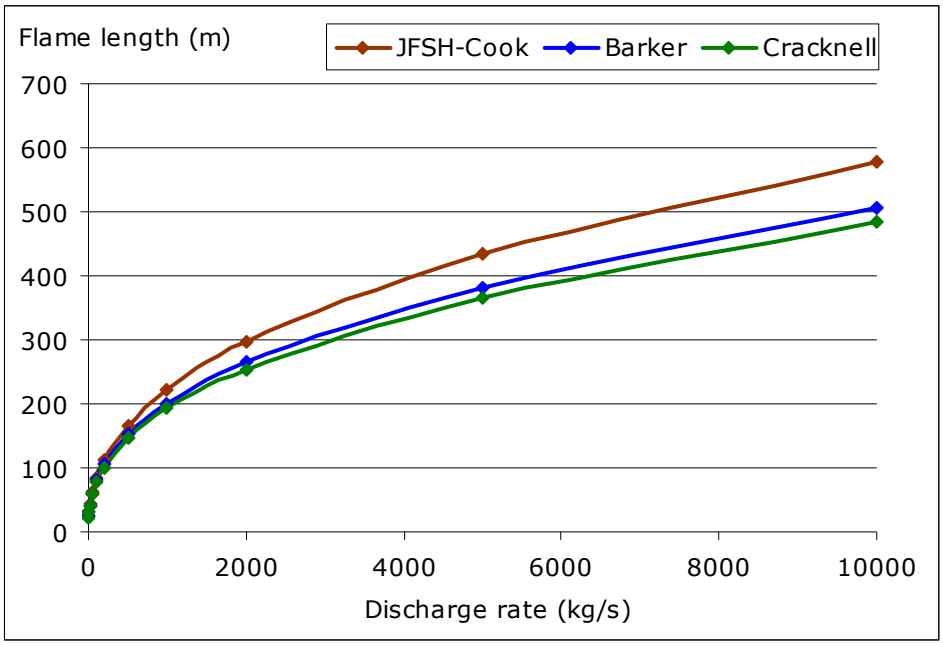

Figure 18 Predicted flame length for discharge rates outside the validation range.

Based on more than 150 experimental releases of methane, propane, butane, crude oil and other hydrocarbons, Lowesmith et al. ([20]) have proposed a general formula for the calculation of the 'jet fire length'[4]: $2.8893 \bullet Q^{0.3728}$, where Q is the total combustion power in MW. The correlation depends on combustion power alone, not on wind conditions or release direction, and is intended to be a good rule of thumb (no more, no less). The Lowesmith flame length correlation is shown in Figure 19[5].

The following remarks are made with respect to the flame length correlation and the underlying data as presented by Lowesmith et al. ([20]):

- The outflow conditions varied widely between the 150^{+} experimental jet fires. Most importantly, the data set included both horizontal and vertical releases. The wind speed and wind direction (relative to the release direction) also varied between the releases.
- The methane and propane flame length data show some scatter. For some release rates, the maximum reported flame length is twice the minimum reported flame length. However, about 70% of the data points are within 20% of the Lowesmith correlation. Especially in the light of the simplicity of the Lowesmith correlation, the methane and propane data fit the correlation well. The highest release rate was nearly 4000 kg/s for methane and 20 kg/s for propane.
- For the mixtures of butane and natural gas, kerosene and natural gas and crude oil and natural gas, the scatter in the observational data is comparable to that of methane and propane. About 80% of the data

4 A precise definition of the term 'jet fire length' is missing in [20]. In personal communication Ms Lowesmith explained that it is the distance from the release point to the flame tip. The 'total combustion power' is not defined in [20] either. We presume that the entire liquid content adds to the combustion power.

5 The actual Lowesmith correlation depends on combustion power. In Figure 19 the combustion energy of butane was used to plot the flame length against release rate. For a logarithmic plot, the differences in combustion energy (kJ/kg) between hydrocarbons are irrelevant.

points are within 20% of the Lowesmith correlation. The highest release rate was close to 5 kg/s.

- For butane, experimental data are available for release rates up to 30 kg/s. It could be argued that the slope of flame length versus power is not as steep as for propane and methane.

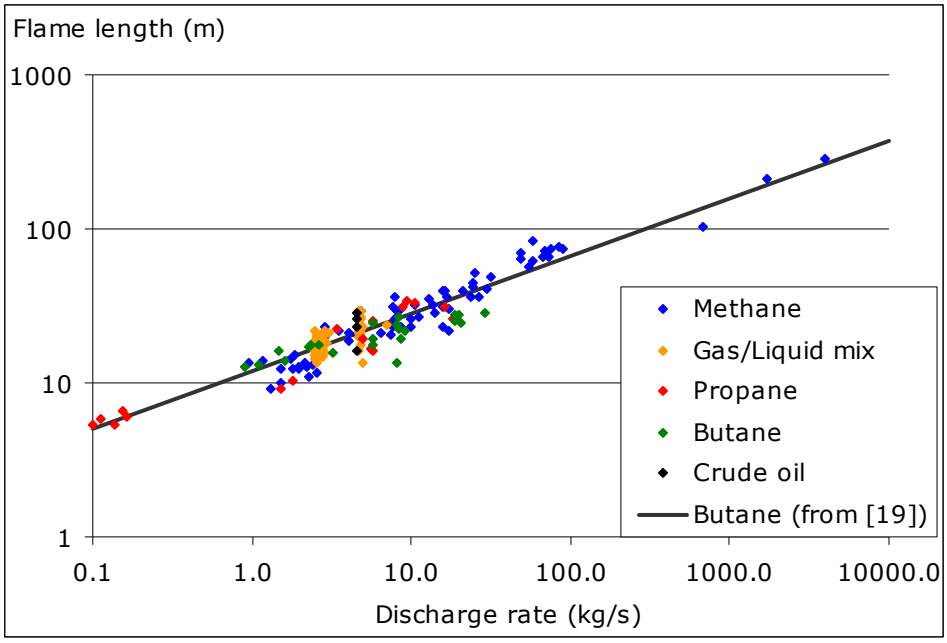

Figure 19 Lowesmith data for flame length.

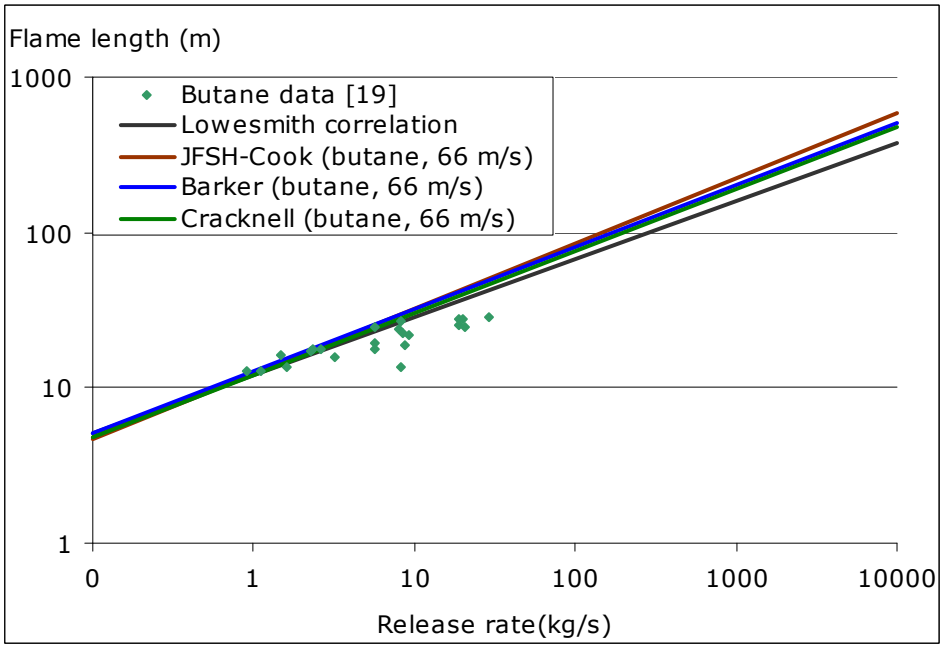

Figure 20 Predictions for butane in comparison with observational data from [20].

In Figure 20, the modelled outcomes for butane jet flame length are plotted along with the experimental data for butane and the Lowesmith correlation for butane. For small release rates, there is little difference between the observed

flame lengths and the calculated values. Between 20 and 30 kg/s, the modelled outcomes are 40 to 60% larger than the observed values. In the extrapolated regime, the JFSH-cook model predicts the largest flame length. The outcome for 10,000 kg/s is 55% higher than the flame length from the Lowesmith correlation. The corresponding outcomes of the Barker and Cracknell models are 35% and 30% higher than the Lowesmith correlation.

In short, given its simplicity, the Lowesmith correlation fits the data surprisingly well. For about 40% of the data points, the correlation yields to an outcome within 10% of the observed flame length. More than 70% of the data points are within 20%. Moreover, the correlation 'performs' just as good for mixtures of volatile and non-volatile components as for pure components.

The selected jet fire models are more sophisticated because in these models the flame length also depends on wind speed and wind direction, release direction and other factors. Whether they also perform better against the observational data could not be tested because the outflow conditions behind the data in [20] were not reported. If the Lowesmith correlation is applied to the selected experiments of section 3.2, the impression is that it performs about as good as the Barker model and Cracknell model and better than the JFSH-Cook model.

4.3.2 Flame height and lift-off

The second aspect that must be addressed is flame height. This height depends on the width of the flame at the tail of the flame and the buoyancy (or lift-off) of the flame near the tail. Figure 17 shows that the predicted flame height and lift-off differ substantially between the models. This subsection discusses which outcome is expected to be most reliable.

The analysis in chapter 3 showed that flame lift-off did occur in the propane and butane releases, but was very limited in the crude oil releases. The explanation was that the high liquid fraction in the crude oil jet increases the density of the jet and that the evaporation of droplets reduces the temperature of the jet. Both effects lead to reduced buoyancy. Therefore, it is argued that flame lift-off will be limited as long as the jet contains a significant amount of liquid.

The selected QRA scenario involves a release of natural gas condensate from a 876 mm (internal diameter) orifice. The considered condensate (Hical) contains 13% very volatile components (C1 to C4), 32% moderately volatile components (C5-C8) and 55% hardly volatile components (≥ C9). The initial pressure is 70 bar(a), but reduces rapidly during the first ten seconds of the modelled release. The time-averaged release rate was calculated at 9483 kg/s (average rate between 0 and 20 s). For these circumstances (high release rates, high amount of non-volatile components), it is expected that a considerable amount of liquid will rain-out. Therefore, if the QRA release scenario would occur, the corresponding flame is expected to be horizontal near the orifice (due to the high jet velocity) while showing buoyancy effects near the tail.

The JFSH-Cook does not take into account flame lift-off and a considerable part of the flame is actually below ground level (see Figure 17). This modelled behaviour is not considered to be representative for the actual flame. The

flame predicted by the Barker model is not expected to be realistic either because lift-off is substantial and occurs too early. At 150 m downwind, the height of the flame is already 140 m. The predicted flame shape is also very narrow (*note once more that the Barker model was not designed for natural gas releases*). Overall, the Cracknell model (showing both a broad flame and lift-off) is assumed to be most reliable with respect to the location of the shape.

4.3.3 Fraction of heat radiated and surface emissive power

The last aspect to be addressed is the amount (or fraction) of heat radiated. Two data sources were used in our analysis:

(i) the previously mentioned publication from Lowesmith et al. [20] which presents data on the fraction of heat radiated for various substances and mixtures;

(ii) results from the JIVE project for mixtures of butane and natural gas ([14]).

In Figure 21 the model outcomes for the fraction of heat radiated are shown in combination with observational data from Lowesmith et al. ([20]):

- The orange triangles correspond to observed values for a various butane jet fires. These data points were taken from Lowesmith et al. ([20]). The release conditions for these data points (e.g. exit velocity) have not been reported.
- The black triangles relate to observed values for crude oil jet fires. These data points were also taken from Lowesmith et al. ([20]). Again, the specific release conditions for these data points were not reported [6].
- The brown line shows the trend calculated with the JFSH-Cook model, using n-butane while keeping the stagnant pressure and release velocity fixed (requested by RIVM, see Annex 3). The open brown diamond at 9483 kg/s represents the data point for the NAM QRA scenario that was discussed in section 4.2.
- The blue line shows the trend calculated with the Barker model, using n-butane while keeping the stagnant pressure and release velocity fixed (requested by RIVM, see Annex 3). The open blue diamond at 9483 kg/s represents the data point for the NAM QRA scenario that was discussed in section 4.2.
- The green line shows the trend calculated with the Cracknell model, again using n-butane, while keeping the stagnant pressure and release velocity fixed (see Annex 3). The open green diamond at 9483 kg/s represents the data point for the NAM QRA scenario that was discussed in section 4.2. For this outcome, a mix of volatile and non-volatile hydrocarbons analogous to the composition of the Hical system was used.
- The purple triangles involve mixed releases of butane and natural gas. These data are borrowed from Figure 4 in Lowesmith et al. ([20]). However, only the releases with a high butane content (between 55 and 85 wgt%) are plotted here. Moreover, the release rate was set at 2.5 kg/s (typical release rate for the JIVE project).

6 The crude oil data were obtained from experiments with stabilised light crude and from oil wells that were ignited in the Gulf war (personal communication with Ms. Lowesmith).

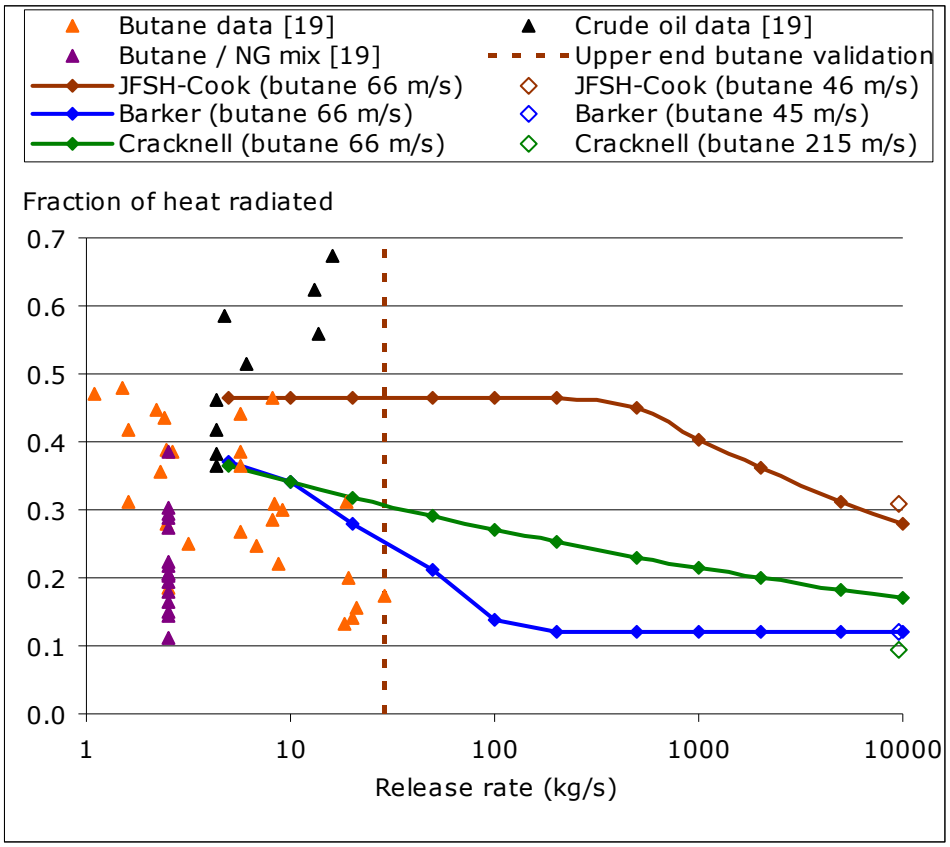

Figure 21 Predicted F-values in combination with Lowesmith et al. data.
(Please note that the x-axis has a logarithmic scale.)

The following remarks are made with respect to the experimental data that are presented in Figure 21:

- The experimental data show a large variation in the fraction of heat radiated. For some release rates, the maximum reported *F*-value could be three times the minimum reported *F*-value. As the outflow conditions behind the data points are unknown, we cannot really say which physical phenomena lie behind the scatter in the data. In section 3.4.2 it was argued that such scattering can derive for example from differences in the exit velocity. The overall average observed *F*-value is 0.32 for butane and 0.5 for crude (see also [20]).
- The data show that on the average, the *F*-value is higher for crude than for butane. This observation is in line with the jet fire literature.
- The highest observed *F*-value (for crude) is around 0.67. This is remarkably high. It would mean that almost all the released fuel would combust (no rainout) and that two-third of the produced energy would be lost by heat radiation (ergo: very limited heating of the combustion products and entrained air).
- The experimental data for butane suggest that the fraction of heat radiated decreases with release rate. However, the number of data points is limited and the outflow conditions of each data point are unknown. Moreover, groups of data points originate from the same set of experiments and cannot be regarded as independent from each other. The apparent decline could be a mere artefact of the limited amount of data. Also, the data points for crude do not show a decline.

- The *fraction of heat radiated appears to be lower* for mixed releases of butane and natural gas than for butane only releases. This is also in line with the literature.
- Lowesmith et al. suggest that the *F*-value of a mixture can be calculated with a linear interpolation between the components (based on mass fractions). However, there is a lot of scatter in the data (see Figure 4 in [20]) and we feel that the interpolation rule is unreliable, especially if the release conditions (release rate, final velocity) deviate from the experimental conditions (which are not reported). If the interpolation rule were applied to the condensate at the NAM site in Den Helder, the outcome would be 0.42 for the Hical mixture and 0.40 for Nogat.

The models behave as follows:
- The JFSH-Cook model starts with a flat line where the fraction of heat radiated is constant (value 0.47). In this region, the amount of heat radiated is derived from the molecular weight and the expanded jet velocity. From 400 kg/s onwards, the *F*-value starts to decrease. The reason is that the surface emissive power is capped in this region by an upper limit of 400 kW/m^2. This point could be seen as the division point between an 'optically thin' and an 'optically thick' regime.
- In the Barker model, the surface emissive power is equal to the limit value of 255 kW/m^2 for all the depicted mass release rates (5 kg/s and higher). In other words, the jet flame is 'optically thick' over the entire range of the graph. The decrease in *F*-value therefore reflects the way in which the ratio of the total flame surface area and the combustion power (release rate) decreases with release rate. A lower bound on the *F*-value is implemented for releases of 100 kg/s and above.
- In the Cracknell model, the behaviour of the *F*-value with increasing release rate is derived from a physical argument and is a function of discharge rate and jet velocity (see section 2.4.1.2). The plotted line merely shows the resulting outcomes. For the Hical scenario (release rate 9483 kg/s, see open green diamond), the fraction of heat radiated was 0,095 and the surface emissive power was 182 kW/m^2.

Given the uncertainty in the data for the fraction of heat radiated, we also investigated if the surface emissive powers that were predicted by the three models were in the right order of magnitude. For the Hical scenario, the Cook model used a SEP of 400 kW/m^2, the Barker model 255 kW/m^2 and the Cracknell model 182 kW/m^2 (see Table 12). Some observational data for mixed butane and natural gas jet fires were provided in the summary report of the JIVE project ([14]). These data are discussed in a little more detail in Annex 4. As can be seen from Figure 35 in Annex 4, the spot surface emissive power increased with butane content. At a somewhat arbitrary spot in the flame, the spot SEP was roughly between 100 and 200 kW/m^2 for a liquid content around 80% (Hical scenario). This increases to values between 150 kW/m^2 and 300 kW/m^2 for intense radiation spots in the flame. The release rates in these experiments were low, between 2 and 3 kg/s.

Reliability of the JFSH-Cook model
The line in Figure 21 is calculated for butane. When compared to the observational data for butane, the calculated fraction of heat radiated (0.47) appears to be conservative. Though the butane data in Figure 21 show substantial scatter, the average *F*-value is about 50% below the JFSH-Cook outcome. Moreover, the JFSH-Cook outcome was calculated for a release with an expanded jet velocity of 66 m/s (see Annex 3). This is a fairly high jet

velocity and as a result, we would expect an *F*-value that is below average, not above average.

For the optically thick regime, the JFSH-Cook model assumes a surface emissive power of 400 kW/m^2. This appears to be conservative, possibly very conservative for large release rates. For example, for the three butane releases in the JIVE project, the highest reported spot surface emissive power was 257 kW/m^2. For all 43 releases in the JIVE project, the highest reported spot SEP was 284 kW/m^2. These releases were limited to 6 kg/s. A lower surface emissive power is expected for (really) high release rates.

RIVM also expressed the desire to use the JFSH-Cook butane outcomes for releases of natural gas condensate. As can be seen from Table 10 and the accompanying notes, these condensates mixtures contain very volatile components (e.g. 5 wgt% methane) and very non-volatile components (e.g. 40% nonane). Without the volatile components, the outcomes would be similar to crude oil. With the methane, the *F*-values will be lower (as can be seen by comparing the butane data to the butane/NG mixture data). Overall it is expected that the resulting *F*-value for a release of 5 kg/s Hical could be anywhere between 0.3 and 0.6 (also depending on the release conditions). The outcome of the JFSH-Cook model (0.46) is in between.

For larger release rates, the heat radiation will be dominated by the surface emissive power. Again, the value of 400 kW/m^2 is expected to be too high. For example, for the crude oil releases of BFETS, the maximum spot surface emissive power was 287 kW/m^2 for BFETS-2 test 1 and 203 kW/m^2 for BFETS-2 test 2. These releases were limited to 5 kg/s. A lower surface emissive power is expected for (really) high release rates.

Reliability of the Barker model
The line in Figure 21 is calculated for butane and starts at 0.37 for 5 kg/s. The Barker outcome appears to be a good approximation of the average value for the (limited number of) butane data points in the plot. If the expanded jet velocity (66 m/s) is accounted for, the calculated value could even be slightly conservative.

For the optically thick regime, the Barker model assumes a surface emissive power of 255 kW/m^2. This value is derived specifically for butane and we have not found any information that showed that this is a significant underestimation or overestimation of the real surface emissive power.

The Barker is not intended to be used for mixtures other than LPG and therefore, we will not compare the outcomes with data for other substances.

Reliability of the Cracknell model
The line in Figure 21 is calculated for butane and starts at 0.37 for 5 kg/s. The Cracknell outcome appears to be a good representation of the average value for the (limited number of) butane data points in the plot. If the expanded jet velocity (66 m/s) is accounted for, the calculated value could even be slightly conservative.

The trend of *F*-value and release rate is derived from a physical argument with additional experimental data. This includes propane and butane releases with a release rate of 25 kg/s and mixtures of butane and natural gas and kerosene

and natural gas at 2.5 kg/s. The (confidential) data show that the outcomes are indeed reliable or possibly conservative for butane (see also Annex A1.3).

The validation for mixtures of gases and liquids is not as convincing as the validation for pure propane and butane. In particular, the fraction of heat radiated might be underestimated in the region between 2.5 and 25 kg/s (see Annex A1.3). Therefore, we recommend expanding the validation range for these mixtures. For release rates above 25 kg/s, the flame will be sufficiently optically thick and we have sufficient confidence that the correlations in the Cracknell model will produce reliable or perhaps even conservative outcomes. For the Hical scenario (release rate 9483 kW/m^2), the resulting SEP is 182 kW/m^2. This appears to be an acceptable value.

Summary
To summarize, the available information in the literature on the fraction of heat radiated is rather limited, especially for materials other than methane. For two-phase releases, the radiated heat depends on the composition, the release rate and the expanded exit velocity, but reliable data could not be found in the public domain. The data points from Lowesmith et al. ([20]) could not be used to test the quality of the selected jet fire models because the outflow conditions behind these data points were not reported.

From a qualitative analysis, the JFSH-Cook model is expected to predict too much heat radiation. The calculated fraction of heat radiated for a 5 kg/s release of butane is probably too high. The maximum surface emissive power that determines the heat radiation in the optically thick regime is also deemed too high.

Using a similar qualitative analysis, it is expected that the Cracknell model gives the most reliable outcomes. Firstly, the fraction of heat radiated is derived from a relatively sophisticated physical argument in combination with experimental data. This validation also includes two-phase mixtures (albeit at low release rates). Secondly, the calculated fraction of heat radiation for a release of 5 kg/s butane at 66 m/s appeared to be quite accurate, possibly even slightly conservative. The fraction of heat radiated in the Hical scenario (0.095) may seem exceptionally low for release of natural gas condensate, but it should be kept in mind that the release rate is extraordinary high.

4.4 Summary and conclusions

In the current chapter, an assessment was made of the reliability of model outcomes for a selected QRA scenario for the Den Helder site of NAM. The QRA scenario involved a release of condensate with a discharge rate of 9483 kg/s (average rate between 0 and 20 s). This discharge rate is far outside the validation range of any jet fire model.

The results of the Barker model are not discussed in this summary because Shell does not recommend its use for these kind of two-phase releases.

The flame length in the Cracknell model is derived from a large experimental data set and appears to be slightly higher in comparison with the Lowesmith et al. correlation for flame length ([20]). The flame length of the JFSH-Cook is validated with a smaller set of data and has a larger deviation with the Lowesmith et al. correlation. Therefore, the flame length predictions of the

Cracknell model are expected to be more reliable than those of the JFSH-Cook model, in particular in the extrapolated range.

With respect to the location of the flame, the JFSH-Cook model predicts a horizontal flame and therefore underestimates buoyancy. The Cracknell model predicts a wide flame with lift-off (angle 21°), which is expected to be more accurate for the type of release considered.

For heat radiation, the differences between the model outcomes were particularly large. The radiated fractions that were observed in experiments showed a lot of variation as well, indicating that this parameter is very sensitive to outflow conditions, such as release rate and exit velocity. For butane releases up to 25 kg/s, the outcomes of the Cracknell model were expected to be more accurate than the outcomes of the JFSH-Cook model. For two-phase releases, the number of validation data behind the Cracknell model was limited and it was uncertain if the predicted heat radiation was accurate between 2.5 and 25 kg/s. The validation data behind the JFSH-Cook model were even more limited, but at least the outcomes appeared to be on the safe side. When extrapolating beyond 25 kg/s, the assumptions behind the JFSH-Cook model will no longer hold and the outcomes will be overconservative. In this region, the physics of the Cracknell model is more reliable. This model is therefore expected to give the best prediction of the fraction of heat radiated in a very large two-phase jet fire.

5 Conclusions

Based on the discussion of outcomes in sections 2.6, 3.4 and 4.4, the following conclusions are drawn:

1. The Barker model and the Cracknell model from FRED are for the larger part derived from experimental outcomes for two-phase and liquid jet releases. Some model assumptions are based on the behaviour of gaseous jets or based on physical arguments. The JFSH-Cook model of SAFETI-NL is derived from a gaseous jet fire model and is validated by a small number of experimental two-phase and liquid releases available in the open literature. The amount of experimental data used to construct the Barker and Cracknell models is significantly larger than the amount of experimental data used to validate the JFSH-Cook model.
2. When compared to the JFSH-Cook model, the Barker model and Cracknell model are more sophisticated. More complex relations are used to determine flame length, flame width, lift-off angle and fraction of heat radiated.
3. The Barker model is intended to be applied to releases of LPG (including pure propane and pure butane) and not for other releases. Indeed, the Barker model produced good results for three selected propane and butane jet fires. It is not recommended to use the Barker model for a release of condensate.
4. Only a limited amount of data is available for jet flames with a mixed gaseous and liquid content. Significant uncertainty pertains to the buoyancy and the fraction of heat radiated of such jet flames. Naturally, the amount of uncertainty is further increased if predictions are made for release conditions well outside the validation range. Some values that are proposed in the literature could be very inaccurate for specific outflow conditions.
5. Between the Cracknell model and the JFSH-Cook model, the Cracknell model is expected to give the better prediction of the flame shape, size and orientation for two-phase and liquid jet fires. For a set of five cases, the Cracknell model overall showed a better match of the flame. The Cracknell model is also considered to be conceptually better because it takes into account buoyancy effects. On the average, the JFSH-Cook model is expected to overpredict the flame length of two-phase and liquid jet fires.
6. Between the Cracknell model and the JFSH-Cook model, the Cracknell model is assumed to predict the amount of heat radiated better. For a set of five cases the Barker model gave slightly better results than the JFSH-Cook model. In the extrapolated range, the JFSH-Cook model relies heavily on a presumed maximum surface emissive power of 400 kW/m^2, which is expected to be overconservative. The Cracknell model is based on more sophisticated physical assumptions and is backed by experimental data. Uncertainties exist however about the predicted heat radiation for two-phase jet fires with a release rate between 2.5 and 25 kg/s. It is therefore recommended to improve the validation behind the Cracknell model for such releases. This is not relevant for the considered QRA scenarios for NAM Den Helder however.
7. Overall, the Cracknell model is expected to produce the best predictions for the NAM Den Helder QRA scenarios. This implies that the flame

length and fraction of heat radiated will be smaller than as predicted by the JFSH-Cook model. This will result in smaller consequence areas and smaller risk contours for the NAM Den Helder site.

References

[1] Besluit externe veiligheid inrichtingen (Decree on External Safety of Establishments), Ministry of Infrastructure and Environment, initially published in 2004, current version 2009.

[2] JFSH Theory Document (part of documentation on PHAST/SAFETI installation CD); DNV; 2005 [confidential].

[3] Developments in design methods for predicting thermal radiation from flares; Chamberlain GA; Chemical engineering research and design; Vol. 65; p.p. 299-309;1987.

[4] A comprehensive program for calculation of flame radiation levels; Cook J, Bahrami Z, Whitehouse RJ; Journal of Loss Prevention in the process industries; Vol. 3; p.p. 150-155;1990.

[5] Large scale natural gas and LPG jet fires - final report to the CEC; Bennett JF, Cowley LT, Davenport JN, Rowson JJ; TNER.91.022; Shell Research Limited; 1991.

[6] Blast and fire engineering for topside structures - phase 2 final summary report; Selby CA, Burgan BA; Steel Construction Institute; 1998.

[7] Flame shape correlations for two-phase jet flames; Barker PWH; Shell Research; 1993. [confidential].

[8] A generalised model for liquid and two-phase jet fires; Cracknell RF; Shell Research; 1996. [confidential].

[9] Interim Guidance Document on the radiation hazards of liquid and two-phase LPG jet fires; Barker PWH; Shell Research; 1994. [confidential].

[10] Large scale natural gas and LPG jet fires - data report for test 3026; Davenport JN, Bennett JF, Cowley LT, Rowson JJ; TNER.91.062; Shell Research Limited; 1991.

[11] Large scale natural gas and LPG jet fires - data report for test 3029; Davenport JN, Bennett JF, Cowley LT, Rowson JJ; TNER.91.063; Shell Research Limited; 1991.

[12] Blast and fire engineering project phase 2 - horizontal jet fires for oil and gas: data report for jet fire test 1; Acton MR, Evans JA, Sekulin AJ; British Gas; 1996.

[13] Blast and fire engineering project phase 2 - horizontal jet fires for oil and gas: data report for jet fire test 2; Acton MR, Evans JA, Sekulin AJ; British Gas; 1996.

[14] Large scale experiments to study horizontal jet fires of mixtures of natural gas and butane; Sekulin AJ, Acton MR; GRC R0367; British Gas; 1995.

[15] Large scale experiments to study horizontal jet fires of mixtures of natural gas and butane - data report for test 8051; Sekulin AJ, Acton MR; GRC R0367 (8051); British Gas; 1995.

[16] Lee's loss prevention in the process industries – hazard identification, assessment and control; S. Mannan (ed.); Third Edition; 2005.

[17] Heat radiation from flares; Guigard SE, Kindzierski WB, Harper N; T/537; University of Alberta; 2000.

[18] Offshore flare design to save weight; Barnwell J and Marshall BK; AIChE meeting; 1984 [referenced in [17], original publication not studied].

[19] Size and radiative characteristics of natural gas flares - part 2 - empirical model; Cook DK, Fairweather M, Hammonds J, Hughes DJ;

Chemical Engineering Research and Design; Vol. 65; p.p. 310-317; 1987. [referenced in [17], original publication not studied].

[20] An overview of the nature of hydrocarbon jet fire hazards in the oil and gas industry and a simplified approach to assessing the hazards; Lowesmith BJ, Hankinson G, Acton MR, Chamberlain G; IChemE Process Safety and Environmental Protection; Vol. 85; p.p. 207-220; 2007.

[21] Controlling hydrocarbon fires in offshore structures; Chamberlain GA; Offshore Technology Conference (6-9 May 2002); OTC 14132; 2002.

[22] Handleiding Risicoberekeningen Bevi, versie 3.2; RIVM; 2009.

[23] Methods for the calculation of physical effects ('Yellow Book'); TNO; 2005.

[24] Formalisation du savoir et des outils dans le domaine des risques accidentels (DRA-35), Ω-8 Feu torche; INERIS; 2003.

Acknowledgement

The authors would like to thank Schelte Rozendal (NAM), Peter Barker (Shell Global Solutions) and Geoff Chamberlain (formerly Shell Global Solutions) for providing the descriptions and data outcomes for the FRED models and for sharing their knowledge on jet fires. Henk Witlox and Adeyemi Oke (both DNV) are acknowledged for the feedback they provided and for their support on the description, validation and application of the JFSH-Cook model.
The authors would further like to thank Michael Acton and Barbara Lowesmith of GL Noble Denton (formerly Advantica) for providing data reports from the BFETS project (phase 2) and for their feedback on various physical aspects of jet fire modelling. The Steel Construction Institute is acknowledged for providing data reports for the JIVE project.

Annex 1 Validation of the models

A1.1 Data used for the validation of the DNV generic two-phase and liquid jet fire model (JFSH-Cook)

The JFSH-Cook model is a modification of the Chamberlain model ([3]). The latter was developed for emergency flaring of pressurised flammable gases. This model was modified by DNV in order to be able to calculate the effects of horizontal jet fires, both gaseous and two-phase ([4]).

To determine and demonstrate the accuracy or validity of the model, DNV has compared public data for several live jet fires with the jet fire model outcomes. The outcomes of this validation are documented by DNV and are available for the users of PHAST and SAFETI-NL. Seven live jet fires from Project AA and BFETS were used for the validation of the two-phase and liquid model. The current project provided additional information for the (five) selected live jet fires. Therefore, the validation was updated in a joint effort by DNV and RIVM.

The outcomes for the flame length are shown in Figure 22. Most predicted values are within 30% of the observed value. The flame length appears to be mildly overpredicted on the average. The largest deviation applies to test 3029 from project AA and test 8051 from JIVE (in both cases about 100% overprediction of flame length).

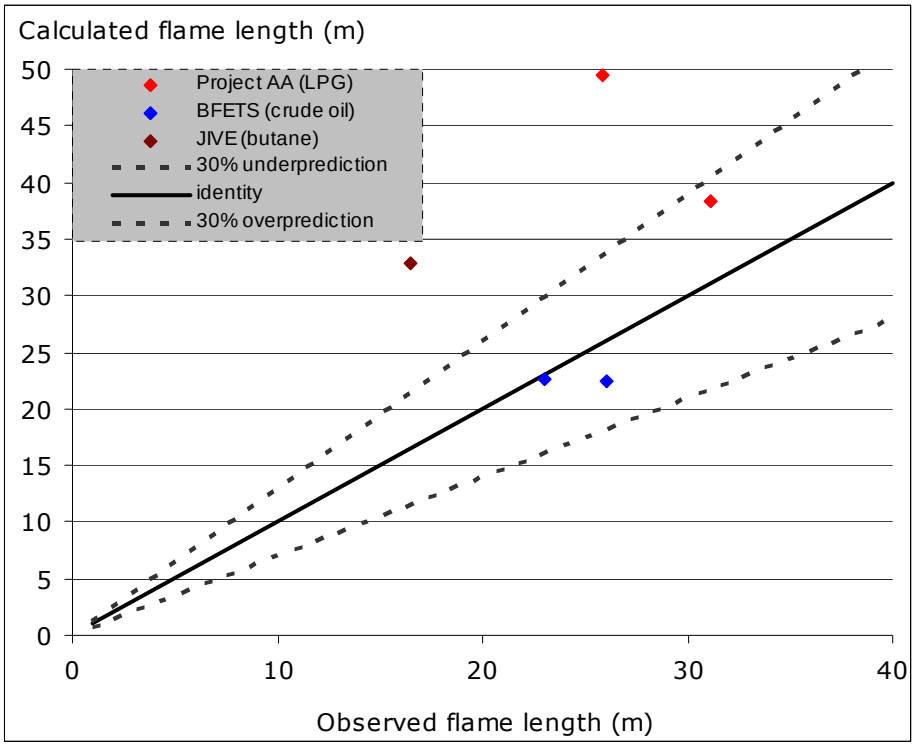

Figure 22 Validation of the flame length (JFSH-Cook model).

The outcomes for surface emissive power are shown in Figure 23. The 'observed' values are presumed to be average values for the Project AA data and maximum values for the BFETS releases. For test 8051 from JIVE the value used in Figure 23 is the average of two spot surface emissive powers that were reported. Because the surface emissive power fluctuates and differs across the flame surface, averages and maximum values cannot easily be measured. Figure 23 should therefore be used with considerable prudence.

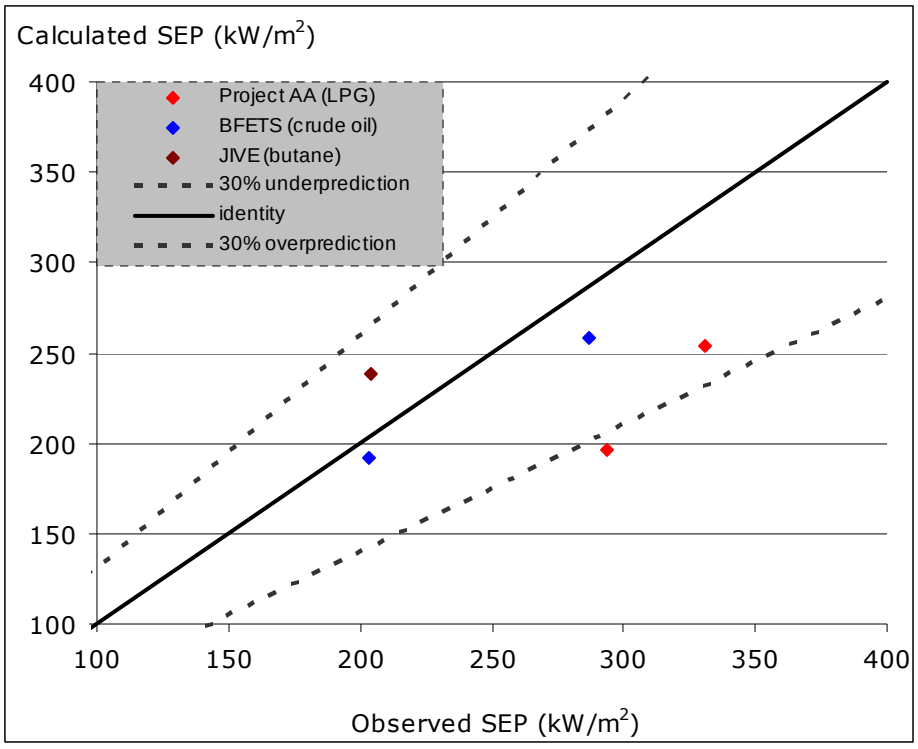

Figure 23 Validation of the surface emissive power (JFSH-Cook model).

A more useful comparison of measured outcomes and modelled outcomes involves the amount of heat radiation that is received at various locations. Such data from radiometers were available for Project Project AA test 3026 and 3029, BFETS-2 test 1 and test 2 and JIVE test 8051. The outcomes are shown in Figure 24. This figure shows that the JFSH-Cook model overpredicts the incident radiation in most cases. Only 10% of the data points have a predicted heat radiation below the observed radiation. 45% of the data points are within 30% of the observed value, 55% within 50% and 80% within 100%. Three data points are extremely far off. These data points are from the JIVE test 8051 and refer to locations along the release axis, 35 m (1×) and 40 m (2×) downstream from the orifice. Figure 14 explains why this large deviation occurs. Without these three data points the average overprediction is 60%, including these data points it is 140% (see Table 13).

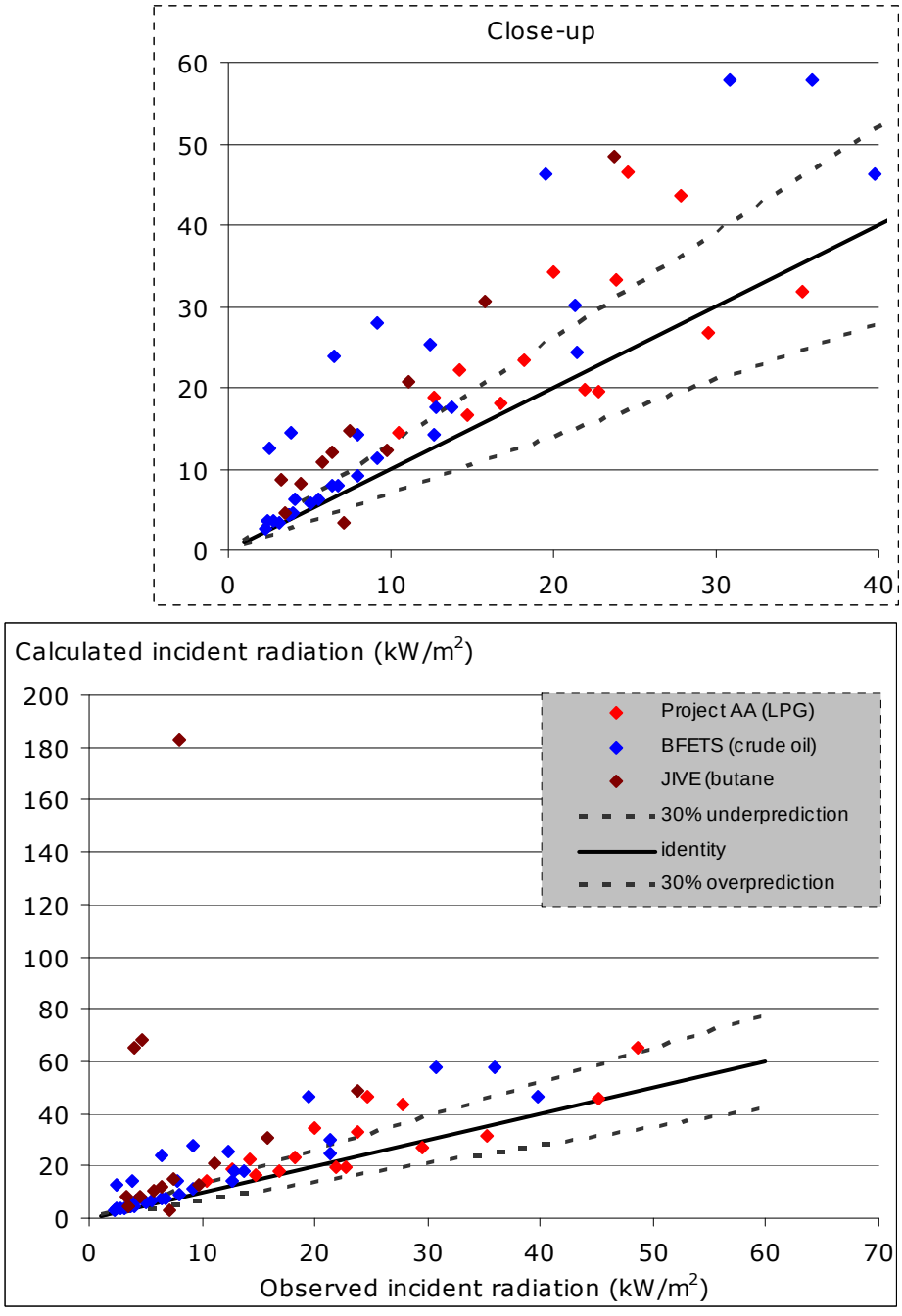

Figure 24 Validation of the incident heat radiation (JFSH-Cook model).

Table 13 Ratio of calculated and observed heat radiation.

	Project AA (propane)	BFETS-2 (crude oil)	JIVE (butane)	All data
Number of data points	15	29	14/11	59/56
Highest value	1.9	5.0	23.0/2.6	23/5.0
Lowest value	0.9	1.1	0.5/0.5	0.5/0.5
Average value	1.3	1.7	5.2/1.7	2.4/1.6

A1.2 Data used for the validation of the Barker LPG jet fire model

The Barker model was developed in the early 1990s by the Shell (Thornton Research Centre). The model was derived from physical arguments and experimental data. The current section takes the original description of the model ([7]) as input. We will therefore speak of the goodness of the fit instead of the quality of the validation. The model has been applied for various live jet fires since its development, but these data were not available to RIVM. As a result of a confidentiality agreement, we will only show the goodness of fit (observed values versus modelled outcomes).

As explained in section 2.3, the flame length is the sum of the length of the horizontal frustum and the length of the tilted cylinder. A dependency on the expanded jet diameter and Froude number was assumed. This dependency was deduced from physical arguments and observations of jet flames in the low momentum regime. The proportionality constant was derived from experiments with propane and butane. Figure 25 shows that the flames that were used to derive the correlation had lengths between 10 and 40 m. Wind did not seem to have a large effect on flame length.

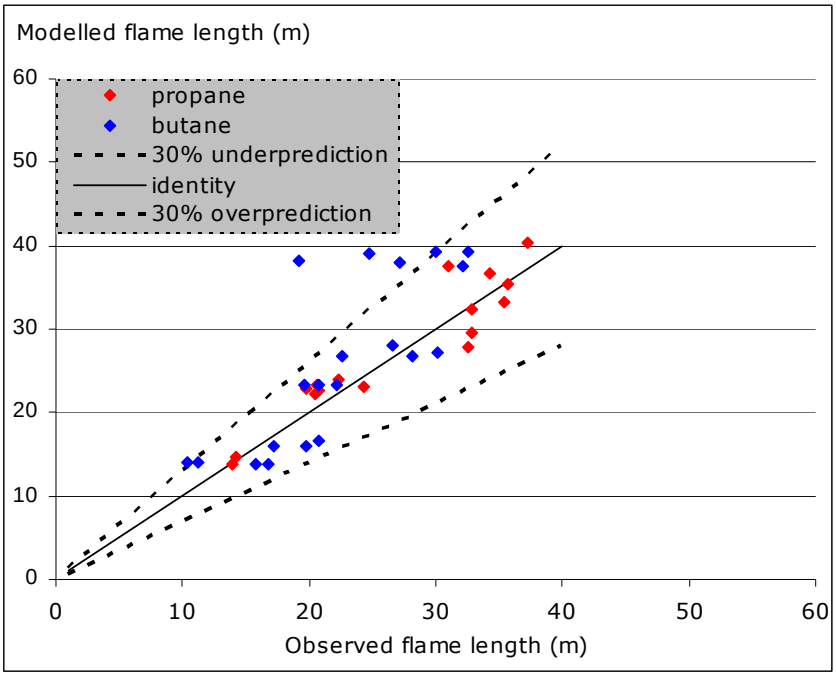

Figure 25 Flame length in the Barker model: goodness of fit

The flame width depends on several source parameters (including release rate, orifice diameter and ambient temperature) and the correlations were also derived from physical arguments. An additional dependency on wind was introduced in the model from experimental data for propane and butane. The wind was mostly in the same direction as the release with speeds between 0 and 7 m/s (two releases had opposing wind with a wind speed between 1 and 2 m/s). The modelled outcomes appear to be slightly larger than the measured values (see Figure 26).

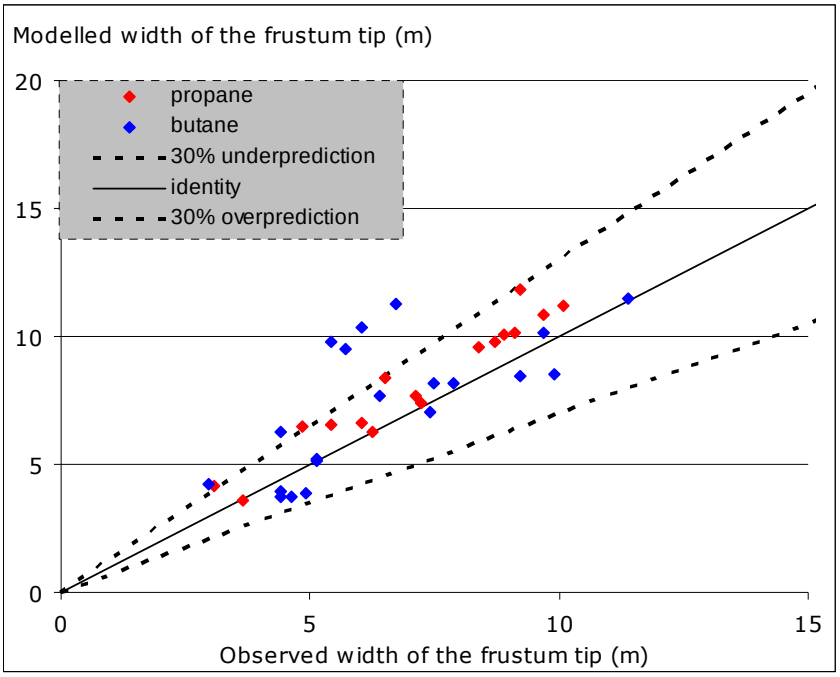

Figure 26 Width of the frustum tip in the Barker model: goodness of fit.

The lift-off angle (Figure 27) was derived from physical arguments for horizontal and vertical velocity. Specific parameter values were derived from experimental data.

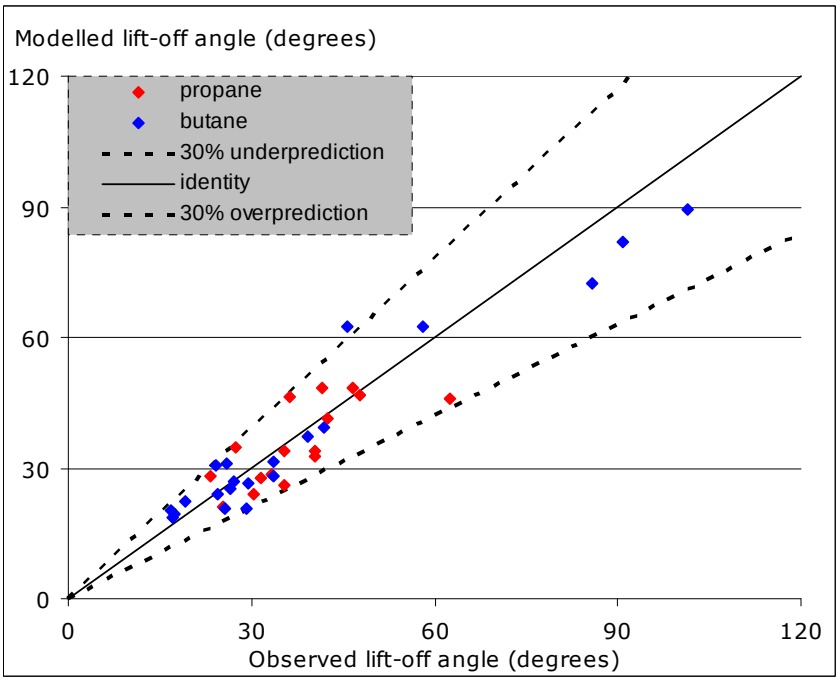

Figure 27 Lift-off angle in the Barker model: goodness of fit.

The surface emissive power (Figure 28) was derived from field radiometer measurements ([9]). For experimental releases, the flame shape according to the Barker model was determined first (in terms of a horizontal cone and a tilted cylinder). Subsequently, it was determined which mean surface emissive

power would reproduce the readings of the field radiometers, taking into account view factors and atmospheric transmissivity. Using this procedure, it was found that the expected mean surface emissive power does not depend on release rate (except for very low release rates). As a result, it was decided to use a conservative value for the surface emissive power in the model calculations (except for very low release rates).

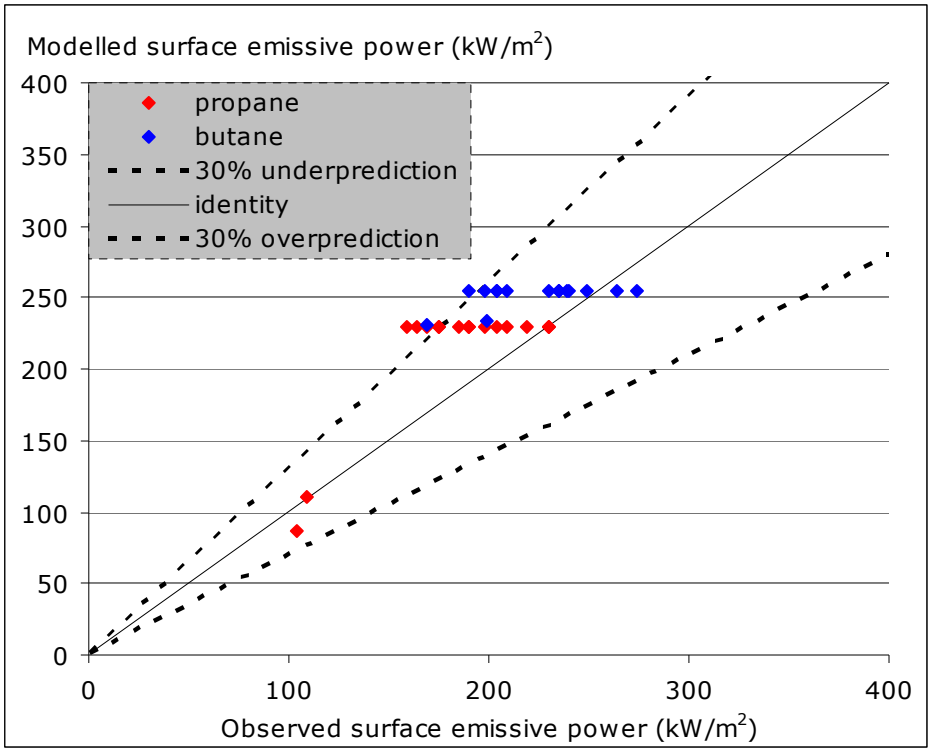

Figure 28 Surface emissive power in the Barker model: goodness of fit.

The fraction of heat radiated is calculated from the surface emissive power, the total flame surface area and the combustion power and is not specifically validated.

A1.3 Data used for the validation of the Cracknell generic two-phase and liquid jet fire model

The Cracknell model was developed in the mid-1990s by Shell (Research and Technology Centre Thornton). Similar to the Barker model, it was derived from physical arguments and experimental data. As a result of a confidentiality agreement, we will only show the goodness of fit (observed values versus modelled outcomes).

In the Cracknell model, the flame length is defined as the length of the straight line between the release point and the end point of the flame centreline. This length is assumed to depend on the mass release rate and the wind velocity relative to the release direction. Mixtures of butane and natural gas and kerosene and natural gas were used to determine the parameters in the correlation. The observed flame lengths for these jet fires were between 10 and 25 m (see Figure 29).

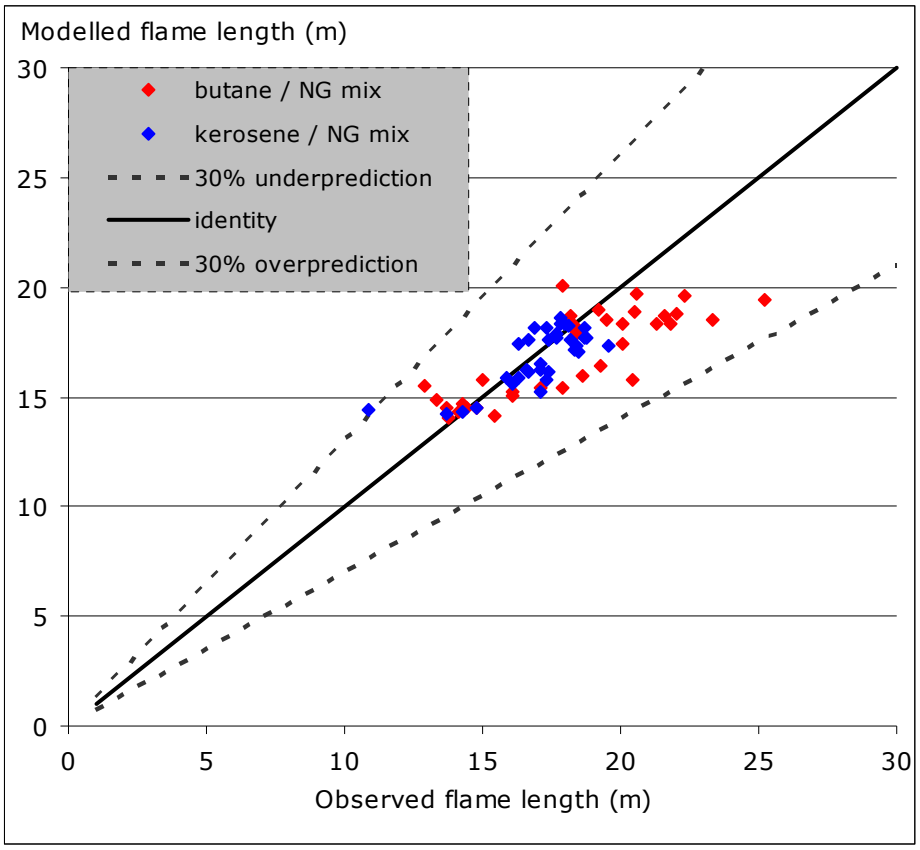

Figure 29 Flame length in the Cracknell model: goodness of fit.

The width of the frustum tip is derived from physical arguments and experimental data for releases of natural gas, propane, propylene, butane with natural gas and kerosene with natural gas. As can been seen from Figure 30, the flame width is overpredicted for propane and underpredicted for the mixture of butane and natural gas. For the other substances the data points generally lie within 30% of the model prediction.

The flame lift-off angle depends on release direction and expanded jet velocity, wind direction and speed and buoyancy. With respect to buoyancy, a physical dependency found earlier for gaseous jet by Chamberlain ([3]) is fitted against data for two-phase jets (propane, butane with natural gas and kerosene with natural gas). The quality of the fit is shown in Figure 31. The amount of scatter in the data is considerable.

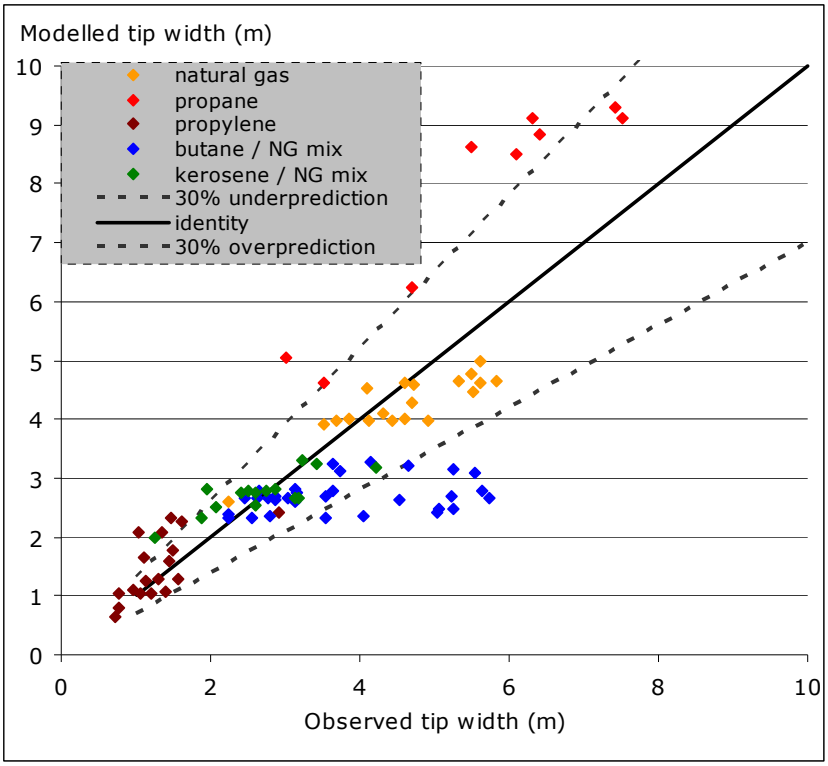

Figure 30 Width of the flame tip in the Cracknell model: goodness of fit.

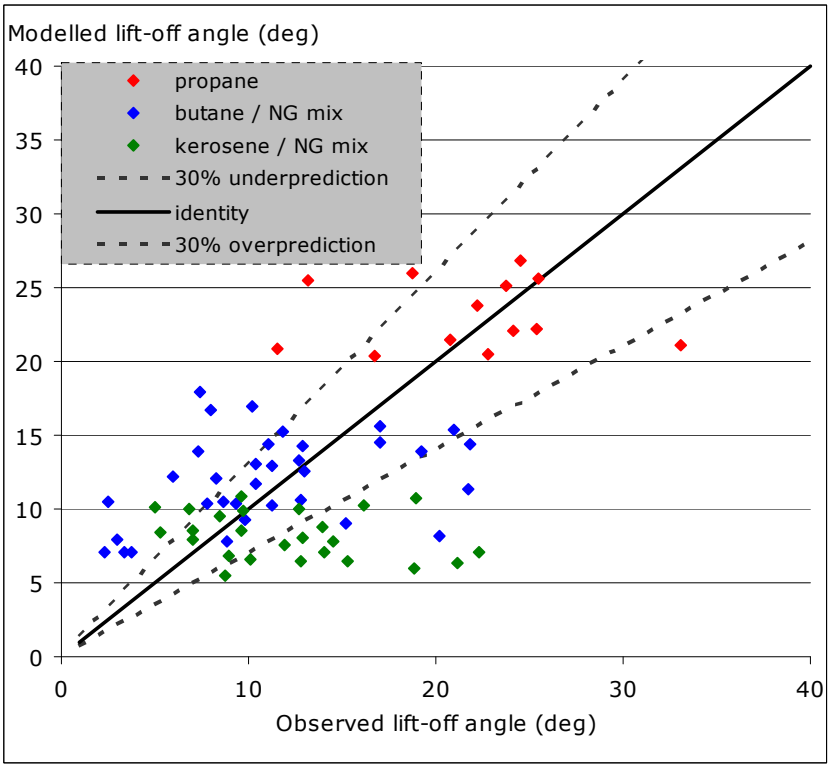

Figure 31 Lift-off angle in the Cracknell model: goodness of fit.

As discussed in section 2.4, the surface emissive power is derived from the fraction of heat radiated (*F*-value). From physical arguments, a dependency of the *F*-value on release rate and jet velocity was deduced. From experiments with propane, propylene and butane and mixtures of butane with natural gas and kerosene with natural gas, it was deduced that the proportionality constant reaches a maximum once the flame becomes optically thick (and no soot is produced). This maximum was taken as an input in the model. As a result, the fraction of heat radiated and the surface emissive power do not depend directly on the released substance (only on expanded jet diameter, velocity and so on).

Almost 100 releases were used for the validation. For 10% to 25% of the data points, the proposed value is lower than the measured outcomes. The assumed maximum is conservative for 75% to 90% of the data points.

For propane, propylene and butane, the release rate was varied and a maximum was indeed visible. The maximum release rate for this validation was 25 kg/s for propane and butane, 0.4 kg/s for propylene. According to RIVM, the confidential data show that the correlation that is used is indeed reliable or even conservative for propane, propylene and butane releases.

For the two-phase mixtures of butane and natural gas and kerosene and natural gas, the composition of the mixture was varied at a constant release rate of 2.5 kg/s. Again the correlation seemed to plateau towards a maximum when the liquid content increased, and this maximum was close to the value obtained for propane, propylene and butane. However, it is not unlikely that the heat radiation of two-phase mixtures is higher at some release rate above 2.5 kg/s. Indeed, the maximum for propane and butane was also observed above 2.5 kg/s. In other words, it is not clear if the maximum that is currently used for two-phase mixtures is indeed the true maximum. We recommend increasing the validation range for two-phase releases up to 25 kg/s. For higher release rates the current value is expected to be sufficiently safe.

Annex 2 Extrapolation of the models

In section 2.5 the influence of the discharge rate on the flame length, the frustum tip width and the fraction of heat radiated, was shown for discharge rates between 0 and 100 kg/s. The models were assumed to be applicable in that particular range. In the current Annex, graphs are shown for discharge rates up to 10,000 kg/s. These values lie outside the validation range of the models, but are nevertheless relevant because the two-phase release rates for the NAM QRA scenarios vary from 5310 kg/s for the Local slugcatcher to 13,332 kg/s for the Nogat slugcatcher. The inputs that were used for these calculations are provided in Annex 3.

Figure 32 shows the length of the jet flame as a function of the release rate. The JFSH-Cook model gives the highest outcomes over the entire range. The difference between the JFSH-Cook model and the other models increase with increasing discharge rate. At the right end of the graph, the predicted value by the JFSH-Cook model is 15% higher than the value predicted with the Barker model and 20% higher than the value predicted with the Cracknell model.

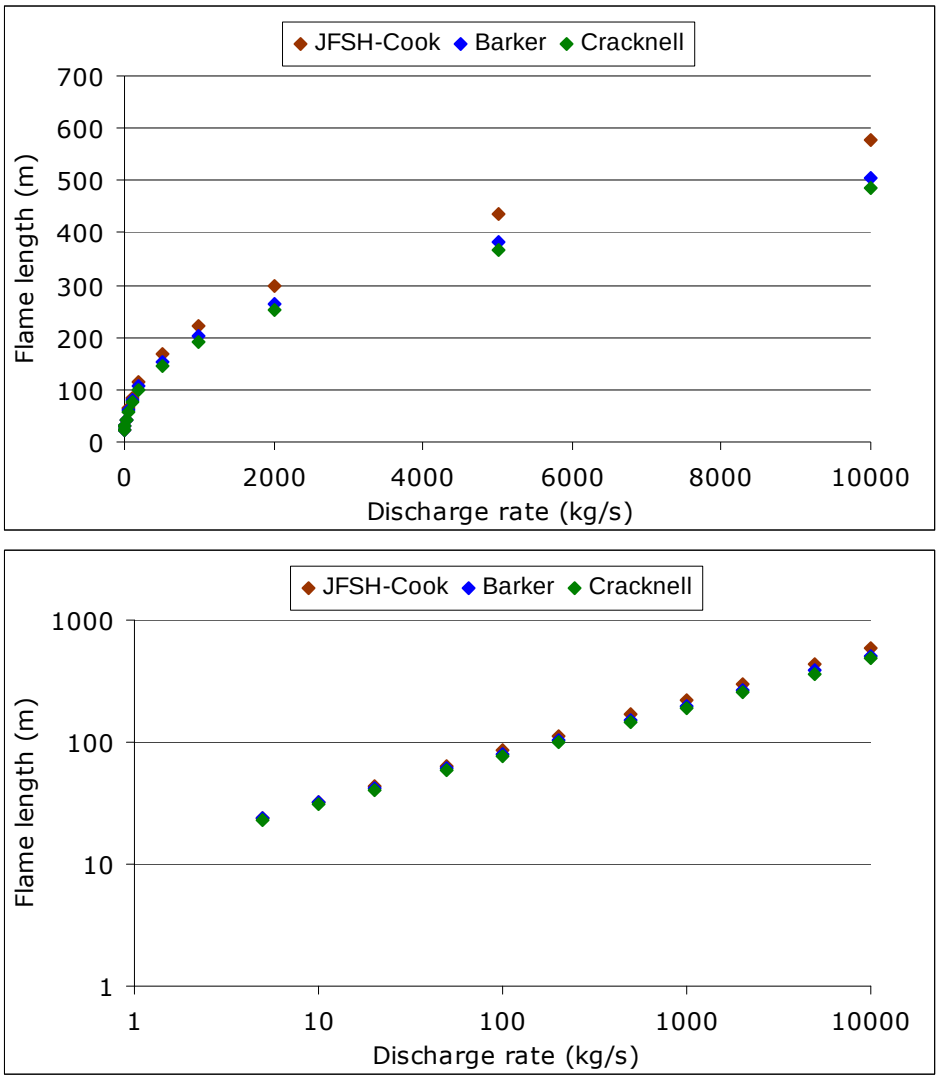

Figure 32 Length of the jet flame as a function of release rate.

Figure 33 displays the width of the frustum tip as a function of the release rate. The differences that were already visible in Figure 6, are magnified in the high release rate regime. The Barker model shows the lowest increase of frustum tip width with release rate, and the Cracknell model the highest increase. From a 1000 kg/s onwards, the JFSH-Cook curve is roughly midway the curves of the two Shell models. As was discussed in section 2.5, a mere comparison of flame width predictions is not very useful.

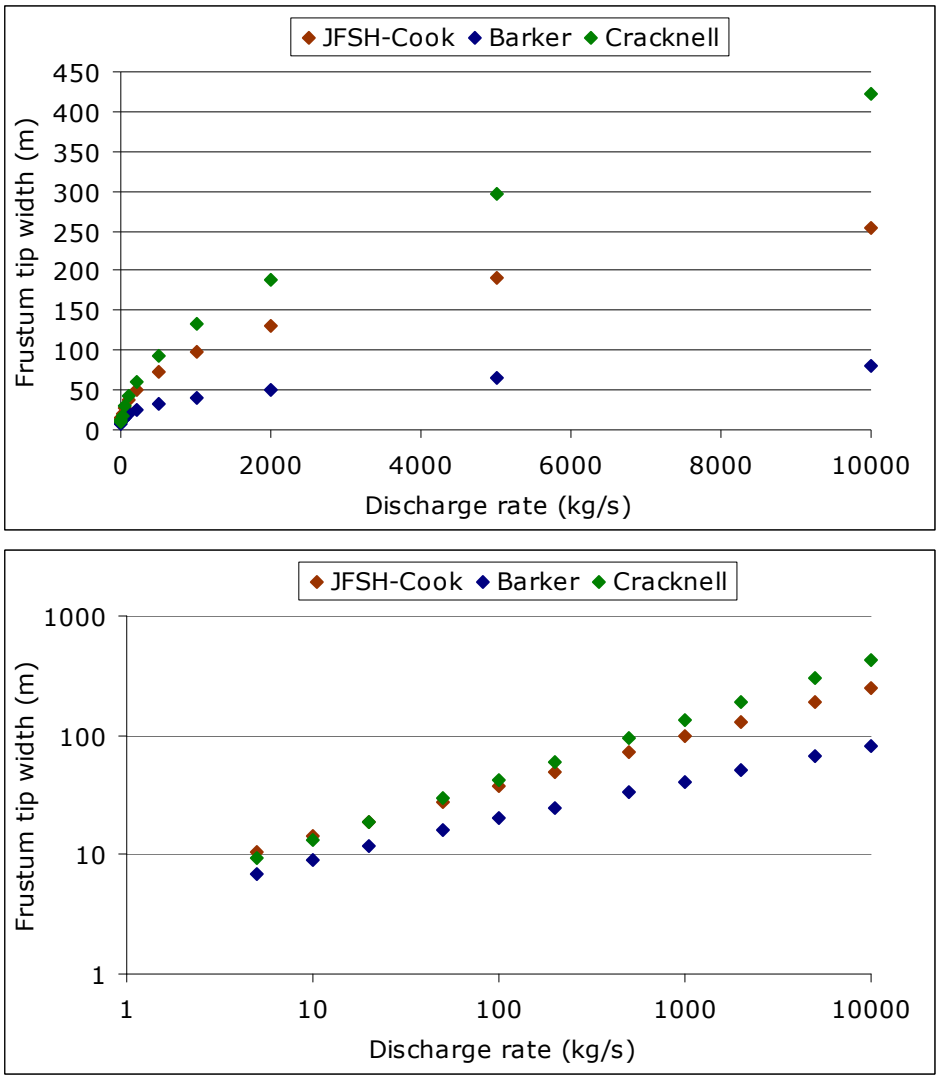

Figure 33 Width of the frustum tip as a function of release rate.

The dependence of the fraction of heat radiated on the discharge rate is shown in Figure 34. For 100 kg/s onwards, the outcome for the Cracknell model is 100% higher than the outcome from the Barker model. At 10,000 kg/s, the difference has reduced to 42%. In the JFSH-Cook model, the fraction of heat radiated remains constant up to 200 kg/s. The emissivity drops from 400 kg/s onwards as a result of an upper bound in the surface emissive power. The predicted values remain considerably higher than the values predicted by the Shell models. At the right end of the graph, the emissivity from the JFSH-Cook (0.28) is 63% higher than the emissivity from the Cracknell model (0.17), and 130% higher than the value from the Barker model (0.12).

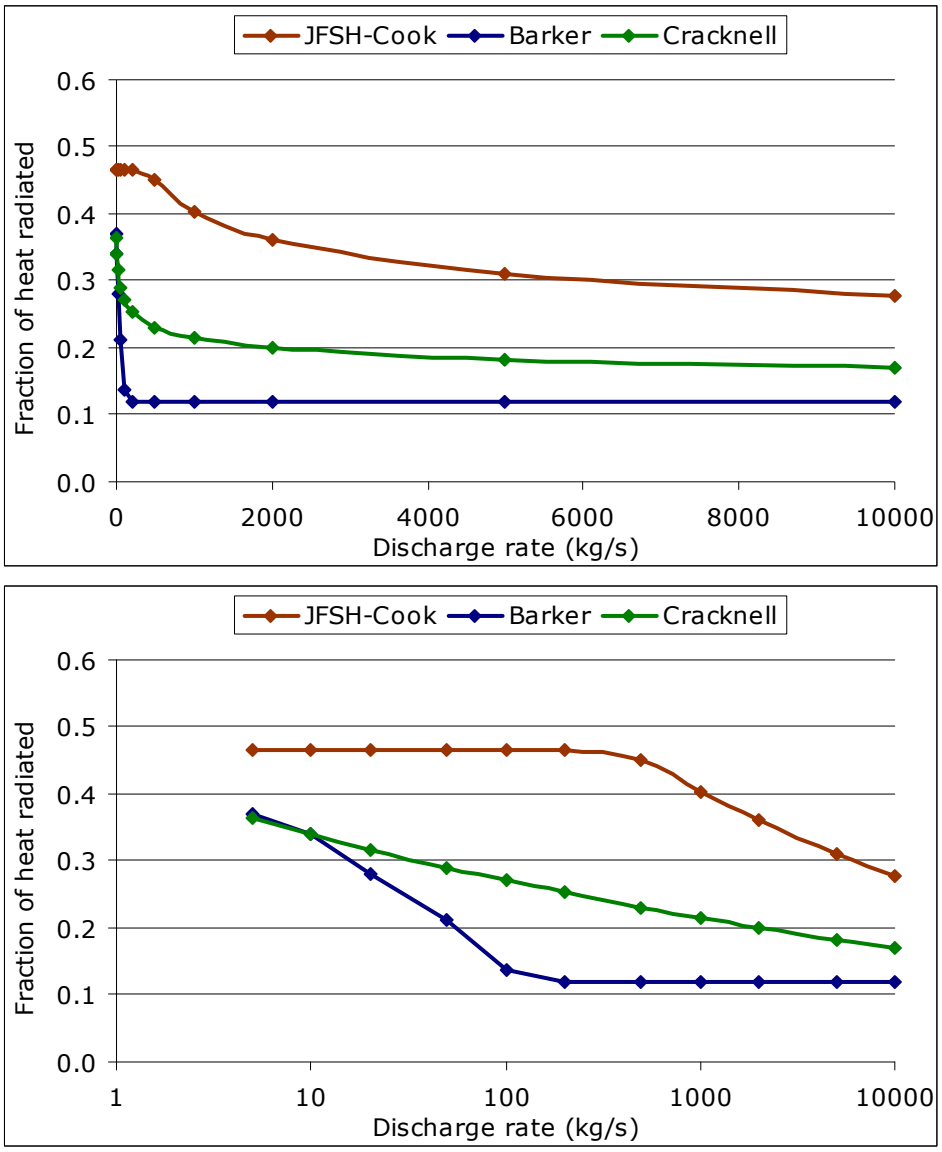

Figure 34 Fraction of heat radiated as a function of discharge rate.

Annex 3 Assumptions and parameter choices used for the illustration of the model behaviour

In section 2.5, the quantitative behaviour of the selected jet fire models was illustrated with six plots. These plots showed the flame length, the width of the frustum tip and the fraction of heat radiated, as a function of the release rate and the expanded jet velocity. Illustrations for extrapolated discharge rates were shown in section 4.3 and Annex 2. This Annex describes the assumptions and parameter choices that were used to generate the plots.

Definition of terms
The 'flame length' is defined as the shortest distance between the orifice and the centre of the tip of the flame. The 'width of the frustum tip' and 'fraction of heat radiated' are self-explanatory.

Requirements for plots showing dependence on release rate
For the plots showing the dependence on the release rate, the following assumptions were used:

i. The release is from a hole in a vessel (discharge coefficient 0.6).
ii. The released substance is 100% n-butane.
iii. No time-dependence is taken into account. Flame properties are derived from the initial release rate.
iv. The stagnant temperature in the tank is 9 °C.
v. The release is from the bottom of the tank and 4 m above ground. The liquid head above the orifice is 3 m.
vi. The expanded jet velocity is 65.87 m/s and the expanded jet temperature 0.47 °C. The liquid fraction after expansion to atmospheric pressure is 0.94. In order to obtain this expanded jet velocity, the stagnation pressure may be varied, but shouldn't deviate much from 10 bar(g).
vii. The release is horizontal and along the wind direction.
viii. The wind speed is 5 m/s at a reference height of 10 m.
ix. The weather is neutral, Pasquill-Gifford class D.
x. The atmospheric temperature is 9 °C, atmospheric pressure 101550 Pa, and humidity 70%.

The release rate is varied by changing the orifice diameter. This shouldn't affect the parameters listed above.

For the plots of section 2.5, section 4.3 and Annex 2, the following set of release rates were used:

- 5 kg/s
- 10 kg/s
- 20 kg/s
- 50 kg/s
- 100 kg/s
- 200 kg/s
- 500 kg/s
- 1000 kg/s
- 2000 kg/s
- 5000 kg/s
- 10,000 kg/s

The release rates exceeding 100 kg/s were only used for section 4.3 and Annex 2.

Requirements for plots showing dependence on expanded jet velocity
The requirements for the plots showing the dependence on the expanded jet velocity are almost identical for the requirements for the variation of the release rate (see previous section). The stagnation pressure is varied in order to obtain different expended jet velocities. The releases rate is fixed at 50 kg/s. The hole diameter must be varied in order to obtain the release rate of 50 kg/s.

For the plots of section 2.5 and Annex 2, the following set of expanded jet velocities is used:

- 30 m/s [(1)]
- 50 m/s
- 70 m/s
- 100 m/s
- 130 m/s
- 160 m/s
- 200 m/s

(1) Or else the lowest expanded jet velocity possible for liquefied n-butane at 9 °C.

Annex 4 Summary of the outcomes of the JIVE project

Between July 1992 and December 1993, 43 jet fire experiments were carried out for mixtures of butane and natural gas. These experiments are referred to as the JIVE project (jet-fire interaction with vessels). Reference [14] gives a summary of the project. The most relevant details are listed below:

- The rig was connected with gas and liquid reservoirs at substantial distance (e.g. 80 m for the butane reservoir). The pressures in the gas reservoir and the liquid reservoir were around 20 bar. At least for butane, a substantial pressure drop in the liquid line was observed (e.g. 2 bar near the nozzle for test 8051). The orifice diameter for the release was either 40 mm or 80 mm. With only two exceptions (test 8050 and test 8051), the release rate was between 2.0 and 2.8 kg/s.
- The release direction was horizontal. The angle between the wind and the release that is reported in Table 16 is the angle between the direction towards which the wind is flowing and towards which the released material is going. An angle of 0° means that the wind and the gas/liquid mixture are flowing in the same direction.
- The gas consisted mostly of methane. The specific composition is shown in Table 14. The heat of combustion of the gas mixture was 49.67 MJ/kg.
- The liquid consisted mostly of butane. The specific composition is shown in Table 15. The heat of combustion of the liquid mixture was 45.71 MJ/kg.
- The flame was monitored with a video and an infrared camera. The flame length reported in Table 16 corresponds to the 20% occurrence length of the flame. The image of the flame that was measured with the infrared camera was usually larger than the image obtained with the video camera, in particular for releases with 40% or more liquid content.
- The flame was also monitored with two narrow angle radiometers. One radiometer aimed at a fixed location in the flame, the other radiometer was aimed specifically at a location where the visible flame was intense.
- The radiation of the flame was measured with several field radiometers. These outcomes were not deemed relevant for this annex.

Table 14 Composition of the gas in the JIVE project.

Substance	**Mol%**
Nitrogen	0.43
Methane	94.0
Ethane	5.31
Propane	0.27

Table 15 Composition of the liquid in the JIVE project.

Substance	**Mol%**
Methane	0
Ethane	0.06
Ethene	0.01
Propane	0.59
Propene	0
i-Butane	2.19
n-Butane	95.56
Butenes	0.14
i-Pentane	1.42
n-Pentane	0.03

Table 16 Summary of outcomes of the JIVE project.

Test	Wind speed (m/s)	Wind angle (°)	Gas flow rate (kg/s)	Liquid flow rate (kg/s)	Flame length (m)	Fixed spot SEP (kW/m^2)	Specific spot SEP (kW/m^2)
8001	0.82	7	2.48	0.00	17.5	77	
8002	0.72	25	1.07	0.95	16.5	85	
8004	0.61	60	1.41	0.94	17.5		
8005	1.76	135	2.50	0.00	16.5	78	
8006	2.58	133	1.51	0.69	15.0	108	
8007	3.78	129	1.87	0.69	15.5		
8023	7.31	19	1.82	0.94	18.5	70	103
8024	6.12	16	1.64	0.95	20.0	120	125
8025	5.23	5	2.56	0.00	18.5	107	106
8026	5.67	8	2.00	0.68	21.0	107	141
8027	6.37	10	2.22	0.49	21.0	106	130
8028	5.93	13	2.00	0.51	20.0	100	122
8029	7.72	13	2.12	0.70	21.0	107	142
8030	6.87	16	1.85	0.67	20.5	106	131
8031	8.47	9	1.44	0.95	22.0	108	154
8032	7.38	13	2.46	0.00	18.5	102	108
8033	9.00	15	2.16	0.51	22.0	106	136
8034	8.70	25	2.27	0.50	21.0	102	103
8035	5.16	18	2.58	0.00	17.5	35	
8036	4.77		1.35	0.96	18.0	103	132
8041	5.61	27	1.49	0.96	19.5	107	122
8042	7.67	35	2.45	0.00	16.5	90	87
8043	5.83	43	1.79	0.71	20.0	95	107
8044	3.96	19	2.53	0.00	17.0	108	66
8045	4.01	13	1.49	0.96	19.5	139	56
8046	5.90	12	1.80	0.70	19.5	129	59
8047	6.65	10	1.50	0.95	20.0		114
8048	4.46	19	2.49	0.00	17.0	74	93
8049	7.51	16	1.81	0.71	20.5	81	109
8050	4.19	117	0.00	6.75		207	
8051	0.49	73	0.00	6.86		151	257
8052	2.52	105	0.00	2.52	10.5	207	
8053	4.16	174	0.66	1.97	14.5	148	284
8054	4.46	144	0.53	1.97	13.5	156	207
8055	5.76	164	1.08	1.50	14.5	115	222
8057	6.04	152	1.66	1.04	15.5	85	155
8058	7.07	150	1.59	1.05	15.0	83	219
8059	5.72	146	1.46	1.03	14.5	84	205
8060	4.60	155	0.98	1.53	14.5	133	282
8061	0.78	75	0.58	1.95	17.0		156
8062	1.42	141	0.40	1.98	17.0		172
8063	0.78	151	0.42	2.00	16.0		174
8064	2.56	131	0.42	2.00	15.0		113

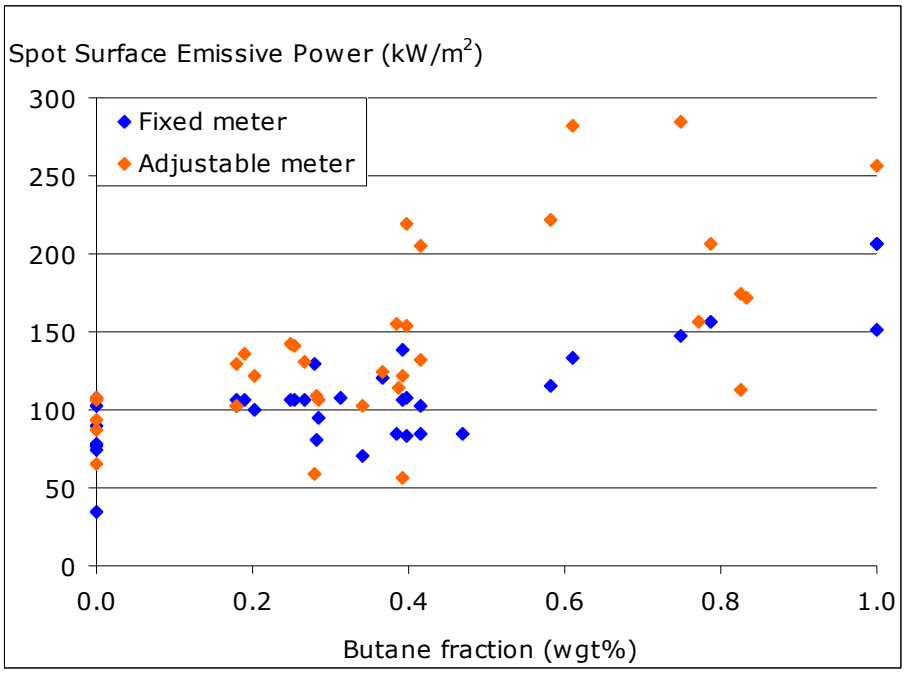

Figure 35 Spot surface emissive power versus liquid fraction (results from JIVE).

National Institute for Public Health and the Environment
P.O. Box 1 | 3720 BA Bilthoven
www.rivm.com